For the published version see https://doi.org/10.1080/00958972.2019.1666980

Synthesis and structural characterization of a barium coordination polymer based on a μ_2-monoatomic bridging 4-nitrobenzoate

Dedicated to Prof. A.V. Salker on the occasion of his 63rd birthday

POOJA H BHARGAO and BIKSHANDARKOIL R SRINIVASAN*
School of Chemical Sciences, Goa University, Goa 403 206, India
Email: srini@unigoa.ac.in

In this report we describe the synthesis, spectra, crystal structure and properties of $[Ba(H_2O)_2(NMF)_2(4\text{-nba})_2]$ **1** (NMF=N-methylformamide; 4-nba = 4-nitrobenzoate).

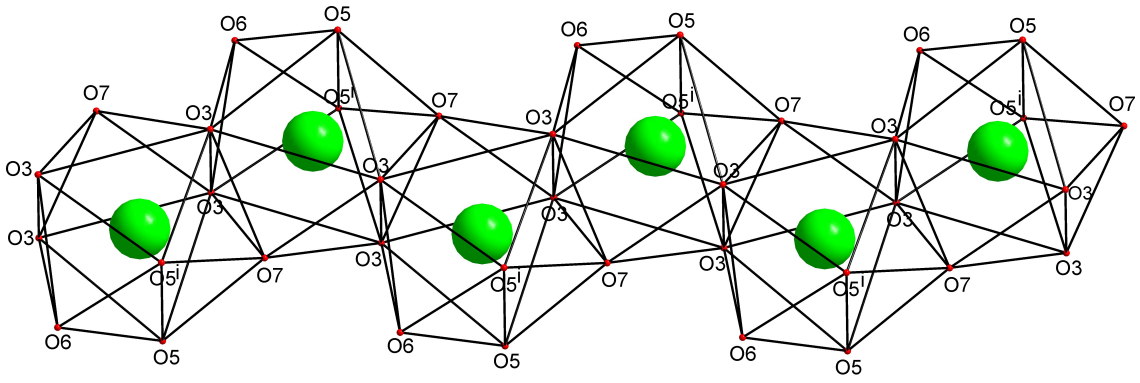

Synthesis and structural characterization of a barium coordination polymer based on a μ_2-monoatomic bridging 4-nitrobenzoate

Dedicated to Prof. A.V. Salker on the occasion of his 63rd birthday

POOJA H BHARGAO and BIKSHANDARKOIL R SRINIVASAN*
School of Chemical Sciences, Goa University, Goa 403 206, India
Email: srini@unigoa.ac.in

Abstract

The synthesis, spectral characterization, crystal structure and properties of $[Ba(H_2O)_2(NMF)_2(4\text{-nba})_2]$ **1** (NMF=N-methylformamide; 4-nba = 4-nitrobenzoate) is reported. ^1H and ^{13}C NMR spectral data reveal the presence of NMF in **1**. A strong band at 1660 cm^{-1} in the infrared spectrum indicates the binding of amide oxygen to Ba(II) which is confirmed by the single crystal structure. The unique Ba(II) in **1** situated on a mirror plane exhibits nine coordination and is bonded to two symmetry related monodentate terminal NMF ligands via the amide oxygen, and a terminal aqua ligand. The μ_2-monoatomic bridging binding mode of each of a crystallographically independent 4-nba ligand and a unique water ligand link the Ba(II) cations into an infinite chain extending along *a* leading to the formation of a one-dimensional coordination polymer with Ba···Ba separations of 4.2522(3) Å. In the chain, the $\{BaO_9\}$ polyhedra are linked in a face sharing fashion. Thermal decomposition of **1** results in the formation of $BaCO_3$ residue. A comparative study of the structural chemistry of several barium coordination polymers is described.

Keywords: Barium; N-methylformamide; 4-nitrobenzoate; μ_2-monoatomic bridging; coordination polymer

1. Introduction

The past decade has witnessed a rapid growth of publications on the chemistry of alkaline-earth metal based materials [1-18]. Of the alkaline-earth metals the heavier congeners starting from Ca are known

to be structurally flexible and exhibit variable coordination numbers while the lighter elements Be and Mg prefer tetra and hexacoordination respectively [1,2]. The bivalent metal barium is known to exhibit coordination numbers ranging from 7 to 12 with nine often being found in many compounds [14-17]. It is well documented in the literature that by using carboxylates ligands, the heavier alkaline-earths starting from Ca can be linked via the bridging binding mode of the carboxylate ligand, into one- or two- or three-dimensional (1D or 2D or 3D) coordination polymers [19-28]. The use of multitopic ligands viz. di- or tricarboxylic acids leads to higher dimensionality (2D and 3D) [23, 30] while many monocarboxylic acids afford a one-dimensional chain polymer [24, 25]. Several examples of barium coordination polymers based on carboxylate ligands have appeared in recent literature [9-15].

A variety of synthetic methodologies [19] ranging from hydrothermal/solvothermal, mechanochemical, sonochemical, gel method, diffusion method etc [30-39]. have been employed by several research groups for compound preparation. However, conventional syntheses performed under ambient reaction conditions in aqueous medium continues to be an often used method [20-29]. In earlier studies, we have demonstrated that an aqueous reaction of readily available reagents viz. substituted benzene carboxylic acid with alkaline-earth metal carbonate is a convenient method for the preparation of coordination polymers of Ca, Sr and Ba [22-23, 40-43]. We have shown that in this acid-base reaction, the insoluble nature of the starting metal carbonate reagent is advantageous both to monitor the course of the reaction and also product isolation. In the case of 4-nitrobenzoic acid (4-nbaH), this reaction readily afforded a 1D coordination polymer containing five terminal aqua ligands, viz. $[Ba(H_2O)_5(4\text{-nba})_2]$ [44] **1a** while zero-dimensional solids of formula $[Mg(H_2O)_6](4\text{-nba})_2\cdot 2H_2O$ [45], $[Ca(H_2O)_4(4\text{-nba})_2]$ [46] and $[Sr(H_2O)_7(4\text{-nba})](4\text{-nba})\cdot 2H_2O$ [47] were obtained for Mg, Ca and Sr respectively. In recent work we have shown that dehydration of the zero-dimensional compound $[Ca(H_2O)_4(4\text{-nba})_2]$ followed by reaction with an O-donor ligand like N-methylformamide (NMF) results in the formation of the anhydrous one-dimensional polymeric compound $[Ca(NMF)_2(4\text{-nba})_2]$ [48]. Application of this strategy to the pentaaqua barium compound **1a** in an effort to enhance its dimensionality resulted in the formation of the water deficient compound $[Ba(H_2O)_2(NMF)_2(4\text{-nba})_2]$

1 containing terminal NMF ligands which exhibits a triple chain polymeric structure. The results of these investigations are described in this paper.

2. Experimental

2.1. Materials and methods

All chemicals used in this study were of reagent grade and were used as received without any further purification. The precursor compound $[Ba(H_2O)_5(4\text{-nba})_2]$ (**1a**) used for the synthesis of **1** was prepared by a literature method [44]. Infrared (IR) spectra of the solid samples diluted with KBr were recorded on a Shimadzu (IR Prestige-21) FT-IR spectrometer from 4000-400 cm^{-1} at a resolution of 4 cm^{-1}. Raman spectra were recorded using 785 nm laser radiations for excitation on an Agiltron Peak Seeker Pro Raman instrument. UV-Visible spectra of aqueous solutions were recorded using a Shimadzu UV-2450 double beam spectrophotometer using matched quartz cells. The photoluminescence spectra were obtained on a xenon flash lamp technology based Cary Eclipse Fluorescence Spectrophotometer (G9800A) from Agilent Technologies. Isothermal weight loss studies were performed in a temperature controlled electric furnace. Elemental analysis (C, H and N) was performed on a Elemental Vario Micro cube CHNS analyzer. TG-DTA study was performed in flowing air in Al_2O_3 crucibles at heating rate of 10 K min^{-1} using a STA-409 PC simultaneous thermal analyzer from Netzsch. ^1H and ^{13}C NMR spectra were recorded using a Bruker 400 MHz (Avance) FT-NMR spectrometer.

*2.2. Synthesis of $[Ba(H_2O)_2(NMF)_2(4\text{-nba})_2]$ **1***

A powdered sample of compound **1a** (0.560 g, 1 mmol) was taken in a beaker and heated in a temperature controlled oven to obtain the anhydrous compound $[Ba(4\text{-nba})_2]$ **1b** in near quantitative yield. The product was cooled to room temperature and an excess of NMF (5 mL) was added into this with stirring to obtain a clear solution which was left aside for crystallization. The crystals of **1** were isolated and washed with ether and air dried. Alternatively, a powdered sample of compound **1a** (0.560 g, 1 mmol) was stirred well to dissolve in NMF (5 mL), and the reaction mixture was left aside for crystallization at room temperature to obtain **1** which was isolated as above.

A mixture of $BaCO_3$ (0.1973 g, 1 mmol) and 4-nbaH (0.334 g, 2 mmol) in water (25 mL) was heated on a water bath for ~30 min to obtain a clear solution. The reaction mixture was filtered and its pH was found to be neutral. The filtrate was concentrated to ~10 mL and NMF (5 mL) was added to it. The reaction mixture was kept undisturbed for crystallization. The crystalline product was isolated by filtration, washed with ether and air dried. (Yield: 75%).

Anal. Calcd for $C_{18}H_{22}N_4O_{12}Ba$ (**1**): C, 34.66; N, 8.98; H, 3.56. Found: C, 34.36; N, 9.17; H, 3.35 %.
IR (KBr, cm^{-1}): 3500-3000(br), 3318(s), 3126(w), 3081(w), 3048(w), 2910(m), 1660(s), 1611(w) 1565(s), 1518(m), 1402(s), 1348(s), 1320(m), 1251(m), 1156(m), 1108(m), 1013(m), 985(m), 958(m), 883(m), 835(m), 794(s), 774(m), 719(m), 514(s).
Raman (cm^{-1}): 3924(m), 3084(w), 2903(w), 1592(s), 1522(w), 1403(m), 1341(s), 1250(w), 1102(m), 957(w), 861(m), 623(w). UV-Vis (in H_2O): 274 nm.
^{1}H NMR (D_2O) δ: 2.63 (s, 3H), 7.86 (d, 2H; J=8.8 Hz), 7.90 (s, 1H), 8.15 (d, 2H, J=8.8 Hz).
^{13}C NMR (100 MHz, D_2O) δ: 24.27(C9), 123.34(C3, C7), 129.45(C4, C6), 142.46(C2), 148.74(C5), 164.74 (C8), 173.51(C1).
DTA (°C): 114 (endo), 190 (endo), 404 (exo), 549 (exo).

2.3. X-ray structure determination

Intensity data for **1** were collected at room temperature on a Bruker Axs Kappa Apex3 CMOS diffractometer with graphite monochromated Mo K_α radiation (λ=0.71073Å) at the Sophisticated Analytical Instrument Facility (SAIF), Indian Institute of Technology (IIT) Madras. The data integration and reduction were carried out using SAINT-PLUS software. The structures were solved by direct methods using SHELXT-2014 and refinement was done against F^2 using SHELXL 2014 [49]. All non-hydrogen atoms were refined anisotropically. All hydrogen atoms attached to the carbon atoms of the aromatic ring of 4-nba and the methyl and amido carbonyl group of NMF ligands were introduced in calculated positions and included in the refinement riding on their respective parent C atoms. The technical details of data acquisition and selected crystal refinement results are summarised in Table 1.

Table 1– Crystal data and selected refinement results for **1**.

Empirical formula	$C_{18}H_{22}N_4BaO_{12}$
Formula weight (g mol^{-1})	623.73
Temperature (K)	296(2)
Wavelength (Å)	0.71073
Crystal system	Orthorhombic
Space group	P*nma*
Unit cell dimensions	

a (Å)	7.3486(3)
b (Å)	31.9323(13)
c (Å)	10.1572(4)
β (°)	90.00
Volume (Å^3)	2383.47(17)
Z	4
D_{calc} (mg/m^3)	1.738
Absorption coefficient (mm^{-1})	1.735
F(000)	1240
Crystal size (mm^3)	0.15 x 0.10 x 0.05
θ range for data collection (°)	3.422 to 25.00
Index ranges	$-8 \le h \le 8$; $-37 \le k \le 37$; $-12 \le l \le 12$
Reflections collected / unique	20066 / 2130 (R(int) = 0.0547)
Completeness to θ	99.8%
Absorption correction	Multi scan
Max. and min. transmission	0.7454 and 0.6374
Refinement method	Full-matrix least-squares on F^2
Data / restraints / parameters	2130 / 3 / 175
Goodness-of-fit on F^2	1.095
Final R indices [I>2sigma(I)]	R1 = 0.0314, wR2 = 0.0671
R indices (all data)	R1 = 0.0427, wR2 = 0.0712
Largest diff. peak and hole (e Å^{-3})	1.659 & -0.539
CCDC No.	1908263

3. Results and discussion

3.1. Synthesis, spectral and thermal investigations

Dehydration of a pentaaqua compound of Ba(II) $[Ba(H_2O)_5(4\text{-nba})_2]$ **1a** by heating followed by reaction of the anhydrous compound $[Ba(4\text{-nba})_2]$ **1b** with N-methylformamide (NMF) was performed in order to enhance its dimensionality and obtain crystals suitable for X-ray structure determination [Scheme1].

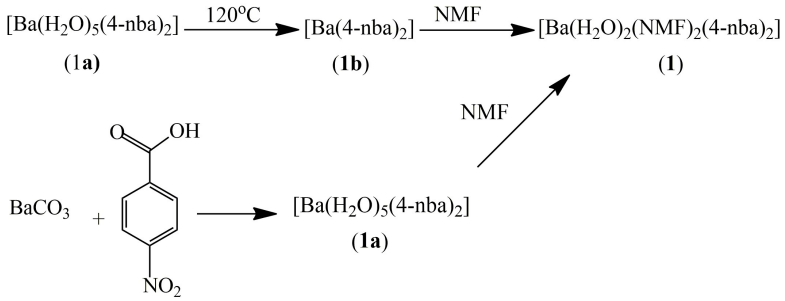

Scheme 1 Synthesis of **1** from **1a**

An excess amide was used to function both as solvent and ligand. The dehydration reaction proceeded as expected, followed by NMF incorporation and crystals of **1** suitable for X-ray study were obtained [Figure S1]. Our efforts to obtain a barium 4-nitrobenzoate compound containing NMF by a direct method under non-aqueous conditions have not been fruitful so far. Hence, it appears that loss or exchange of two aqua ligands from **1a** by NMF probably facilitates its structural reorganization leading to the formation of **1**.

An investigation of the crystalline product by ^{1}H and ^{13}C NMR revealed the presence of NMF in addition to 4-nitrobenzoate as evidenced by the characteristic ^{1}H chemical shifts for the hydrogen attached to the amide carbon and methyl protons of NMF [Figure S2]. The ^{13}C NMR spectrum [Figure S3] exhibits a total of seven signals, five of which can be assigned for the distinct carbons of 4-nba. The signals at 164.7 and 24.3 ppm are characteristic of the amide carbon and the methyl carbon attached to the electronegative N. An intense band at 1660 cm^{-1} which is not present in the precursor **1a** can be assigned for the vibration the amide carbonyl [Figure 1]. In addition, the IR spectrum revealed the presence of water in **1** by a broad signal in the –OH region thus indicating that the final product still contains some water. Since the free NMF ligand exhibits the carbonyl band at ~1690 cm^{-1} it could be inferred that the amide oxygen is bonded to the metal as explained in the crystal structure (*vide infra*).

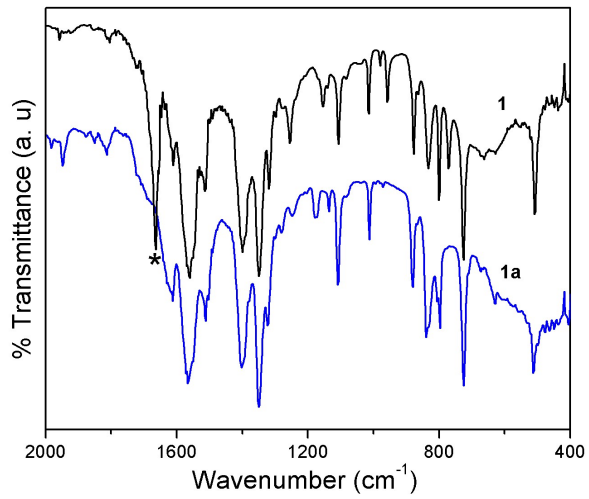

Figure 1 – Infrared spectra of compounds **1** and **1a** in the region 2000-400 cm^{-1}. *Signal of amide carbonyl.

Pyrolysis of the product revealed the chemical composition of Ba:4nba:water:NMF to be 1:2:2:2 indicating that the above synthetic methodology affords a water deficient and not an anhydrous compound. In view of the above, especially the binding of amide oxygen to Ba, the synthesis was performed by a direct dissolution of **1a** in NMF which also afforded **1**. Further, a one-pot synthesis was performed, wherein **1a** was generated *in situ* by an aqueous reaction of $BaCO_3$ with 4-nbaH and further reaction with NMF [Scheme 1] which also afforded the same product as evidenced by identical IR spectra and powder pattern. A comparison of the pattern of the NMF containing compound with that of the precursor pentaaquacompound **1a** [Figure S4] reveals that a new phase is formed which is in good agreement with the pattern calculated from the single crystal data (*vide infra*).

The IR spectrum of **1** exhibits several sharp bands in the mid-IR region, indicating the presence of the organic moieties. The appearance of a feature at ~3318cm^{-1} can be attributed to the –NH stretching vibration of the NMF. A comparison of the IR spectra of the free ligand 4-nbaH, compounds **1a** and **1** reveal the absence of the –COOH signal in **1a** and **1** which is observed at 1690 cm^{-1} in the free acid [Figure S5]. The differing nature of **1a** and **1** is revealed by a change in the profile of the spectra in the –OH region and the observation of an intense amide carbonyl vibration at 1660 cm^{-1} in **1**. Both compounds exhibit an intense signal at around 1350 cm^{-1} which can be assigned for the symmetric stretching vibration of the nitro group of 4-nba. Interestingly, this signal is the most intense band in the Raman spectra of both compounds [Figure S6]. Compound **1** absorbs in the UV region and the spectrum is almost similar to that of 4-nbaH or **1a**. The intense band at 274 nm in the UV-Vis spectrum [Figure S7] can be assigned to the intramolecular charge transfer transition of the 4-nitrobenzoate. The photoluminescence property of **1** was investigated by exciting a powdered sample of **1** with 280 nm radiation using an excitation slit width of 10 nm and an emission slit width of 5 nm at a scan rate of 600 nm per minute. For comparison, the same instrument settings were employed for the study of the free ligand 4-nbaH and the precursor comound **1a** [Figure S8]. The fluorescence emission spectra of all the compounds are very nearly similar with emission at a longer wavelength of 379 nm, which can be assigned to an intraligand $\pi \rightarrow \pi^*$ transition of the 4-nitrobenzoate ligand.

Compared to the free ligand, the fluorescent intensity is diminished in **1,** which indicates that binding of 4-nba to the closed shell Ba(II) does not bring about any major changes excepting in a reduction in the emission intensity. It is interesting to note that the fluorescence emission of the pantaaqua Ba(II) compound **1a** is almost the same as the free ligand but slightly more than that of **1** [Figure S8].

Isothermal weight loss analysis of the compound at 100°C showed a mass loss of 15.24% which is much more than the value (5.72) expected for the loss of two moles of water and less than that expected for the loss of 2 NMF (18.9). An IR spectral analysis of **1** heated at 100°C reveals the loss of amide in addition to water as evidenced by a diminishing of the intensity of the amide carbonyl signal [Fig S9]. Hence this mass loss can be assigned for the loss of two H_2O molecules and also for a partial loss of NMF ligands. It is observed that heating at 120°C results in a total disappearance of the amide carbonyl peak [Fig S9]. Pyrolysis of the bulk compound performed in a temperature controlled furnace at 800°C results in the formation of 31.55% of residual $BaCO_3$, which is in good agreement with the theoretical value of 31.64%. The formation of carbonate residue was inferred by a characteristic spot test for carbonate. The TG-DTA curves add more credence to the thermal behavior of **1**. The TG curve exhibits two endothermic events at 114°C and 190°C, respectively [Fig S10] and the total mass loss of ~25% is fairly in agreement with the loss of aqua and NMF ligands. The DTA curve displays two exothermic events at 404°C and 549°C, which can be due to the degradation of the carboxylate moieties leading to decomposition of compound **1**. It is to be noted that in many alkaline-earth 4-nitrobenzoates exothermic events have been observed above 400°C [44-47]. The observed residual $BaCO_3$ of 29.12% in the TG experiment is slightly less than that of the expected value.

3.2. Description of crystal structure

Compound **1** crystallizes in the centrosymmetric orthorhombic space group *Pnma* with Ba1, O6 and O7 located on a mirror plane and all other atoms situated in general positions. In view of the special position of the central metal and the aqua ligands, the asymmetric unit of **1** having molecular formula $[Ba(H_2O)_2(NMF)_2(4\text{-nba})_2]$ consists of an unique Ba(II) ion, a crystallographically independent 4-nba ligand, a unique terminal NMF ligand, and two crystallographically unique aqua ligands O6 and O7

respectively [Figure S11]. The geometric parameters of the NMF and 4-nba ligands are in the normal range [Table S1].

The central barium exhibits nine coordination [Figure 2] and is bonded to two symmetry generated terminal NMF ligands via the amide oxygen O5, a terminal aqua ligand O6, and four symmetry related 4-nba ligands via O3 and to two symmetry related water molecules O7 resulting in a distorted monocapped square antiprismatic $\{BaO_9\}$ polyhedron [Figure 2]. The Ba-O bond distances vary between 2.749(3) and 2.953(4) Å in **1** [Table 2] while the O-Ba-O bond angles range from 64.65(9) to 142.29(6)°. These values are in good agreement with reported data for other barium coordination polymers [23, 44, 57, 58].

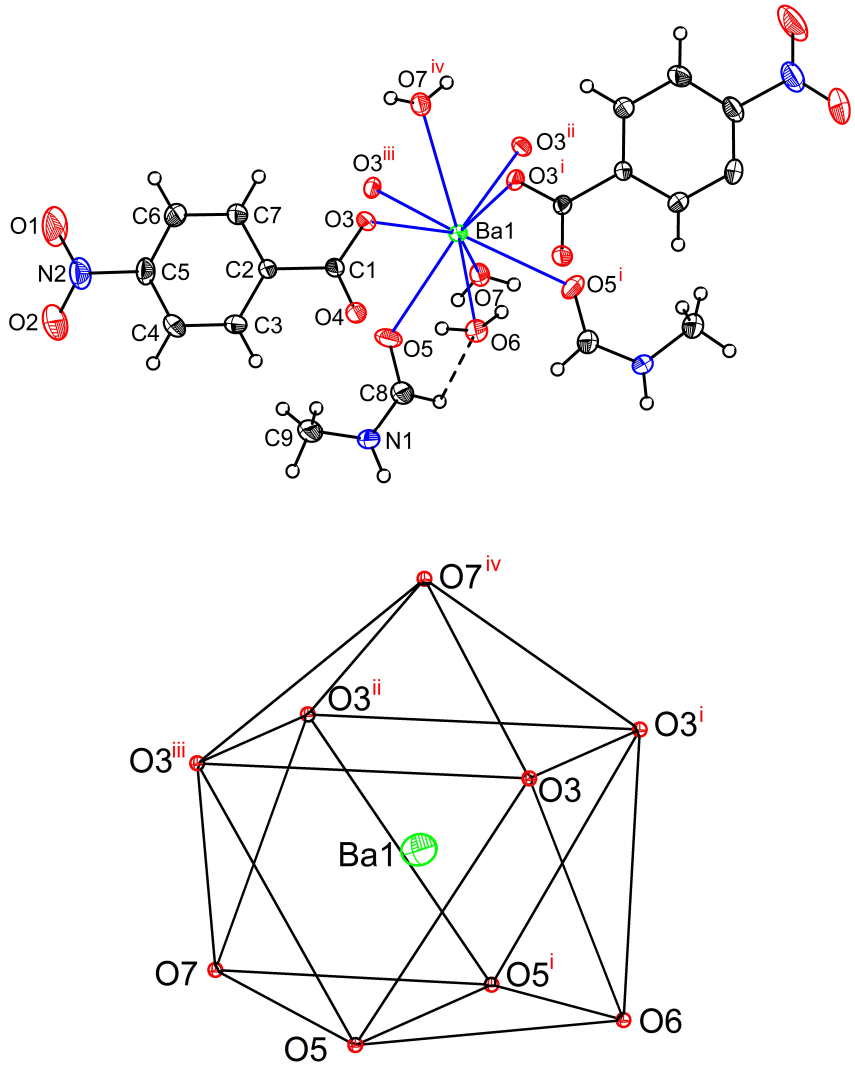

Figure 2 – The crystal structure of $[Ba(H_2O)_2(4\text{-nba})_2(NMF)_2]$ (**1**) showing the atom labelling scheme and the coordination sphere of Ba(II) in **1** (**Top**). Displacement ellipsoids are drawn at the 30% probability level excepting for the H atoms, which are shown as circles of arbitrary radii. The distorted monocapped square antiprism $\{BaO_9\}$ coordination polyhedron in **1** (**Bottom**). Symmetry code: i) x, -y+1/2, z ii) x-1/2, -y+1/2, -z+1/2 iii) x-1/2, y, -z+1/2 iv) x+1/2, y,-z-1/2.

Table 2 – Selected bond lengths and bond angles of $[Ba(H_2O)_2(NMF)_2(4\text{-nba})_2]$ (**1**).

Bond lengths (Å)			
Ba1-O5	2.749(3)	Ba1-O5^{i}	2.749(3)
Ba1-O7	2.768(5)	Ba1-O3^{i}	2.803(3)
Ba1-O3	2.803(3)	Ba1-O3^{ii}	2.782(3)
Ba1-O6	2.923(5)	Ba1-O3^{iii}	2.782(3)
Ba1-O7^{iv}	2.953(4)	Ba···Ba^{i}	4.2522(3)
Bond angles (°)			
O5-Ba1-O5^{i}	98.39(14)	O3^{ii}-Ba1-O3	132.50(4)
O5-Ba1-O7	70.95(10)	O3^{iii}-Ba1-O3	87.03(6)
O5^{i}-Ba1-O7	70.95(10)	O3^{i}-Ba1-O3	73.87(11)
O5-Ba1-O3^{ii}	136.67(9)	O5-Ba1-O6	66.55(9)
O5^{i}-Ba1-O3^{ii}	79.11(9)	O5^{i} -Ba1-O6	66.55(9)
O7-Ba1-O3^{ii}	67.41(9)	O7-Ba1-O6	112.52(13)
O5-Ba1-O3^{iii}	79.11(9)	O3^{ii}-Ba1-O6	142.29(6)
O5^{i}-Ba1-O3^{iii}	136.67(9)	O3^{iii}-Ba1-O6	142.29(6)
O7-Ba1-O3^{iii}	67.41(9)	O3^{i} -Ba1-O6	71.79(9)
O3^{ii} -Ba1-O3^{iii}	74.50(11)	O3-Ba1-O6	71.79(9)
O5-Ba1-O3^{i}	135.38(9)	O5-Ba1-O7^{iv}	130.74(7)
O5^{i}-Ba1-O3^{i}	78.59(9)	O5^{i} -Ba1-O7^{iv}	130.74(7)
O7-Ba1-O3^{i}	143.06(5)	O7-Ba1-O7^{iv}	122.89(12)
O3^{ii} -Ba1-O3^{i}	87.03(6)	O3^{ii}-Ba1-O7^{iv}	67.86(9)
O3^{iii}-Ba1-O3^{i}	132.50(4)	O3^{iii} -Ba1-O7^{iv}	67.86(9)
O5-Ba1-O3	78.59(9)	O3^{i}-Ba1-O7^{iv}	64.65(9)
O5^{i}-Ba1-O3	135.38(9)	O3-Ba1-O7^{iv}	64.65(9)
O7-Ba1-O3	143.07(5)	O6-Ba1-O7^{iv}	124.59(13)

Symmetry transformations used to generate equivalent atoms: (i) x, -y+1/2, z
(ii) x-1/2, -y+1/2, -z+1/2 (iii) x-1/2, y, -z+1/2 (iv) x+1/2, y, -z+1/2.

It is interesting to note that the amide oxygen O5 of NMF makes the shortest bond (Ba-O5 = 2.749(3) Å) which is shorter than the Ba-O bond length of the terminal water O6. Unlike O6, the second unique water O7 functions as a μ_2-bridging bidentate ligand [Figure S12] and is bonded to a Ba at 2.768(5) Å; O7 makes another contact with a second Ba(II) at a longer distance of 2.953(4) Å accompanied by a Ba···Ba separation of 4.2522(3) Å. As a result of this bridging binding mode of O7, the Ba(II) ions are linked into an infinite chain extending along *a* axis [Figure 3].

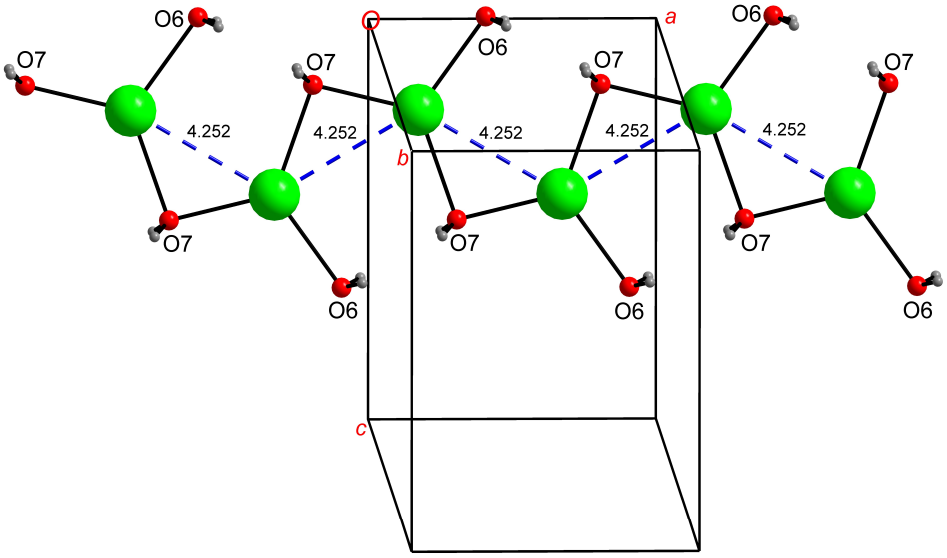

Figure 3–A portion of an infinite chain extending along *a* axis due to the μ_2-bridging bidentate (O7) of aqua ligand in **1**. For clarity, only the terminal aqua ligands around each Ba(II) are shown.

Each Ba(II) in the chain is bonded to three terminal ligands, two of which are O5 of NMF and the third is O6 of water [Figure S13]. The unique 4-nba ligand functions as a monoatomic bridging μ_2-η^2 ligand [Figure S12] and is bonded to two symmetry related Ba(II) ions at Ba-O distances of 2.782(3) and 2.803(3) Å respectively via the O3 of the carboxylate functionality.

In the crystal structure, a pair of such monoatomic bridging 4-nba ligands link a pair of Ba(II) ions and extend the structure along *a* [Figure 4] resulting in a double chain. The net result of the binding of the terminal NMF ligand (O5), terminal aqua ligand (O6) and the bridging 4-nba ligand (O3) and bridging water (O7) is the linking of Ba(II) ions into a triple chain coordination polymer [Figure S14]. Each Ba(II) in the one-dimensional chain carries three terminal ligands and exhibits a separation of 4.2522(3) Å with the adjacent Ba(II) ions on either side.

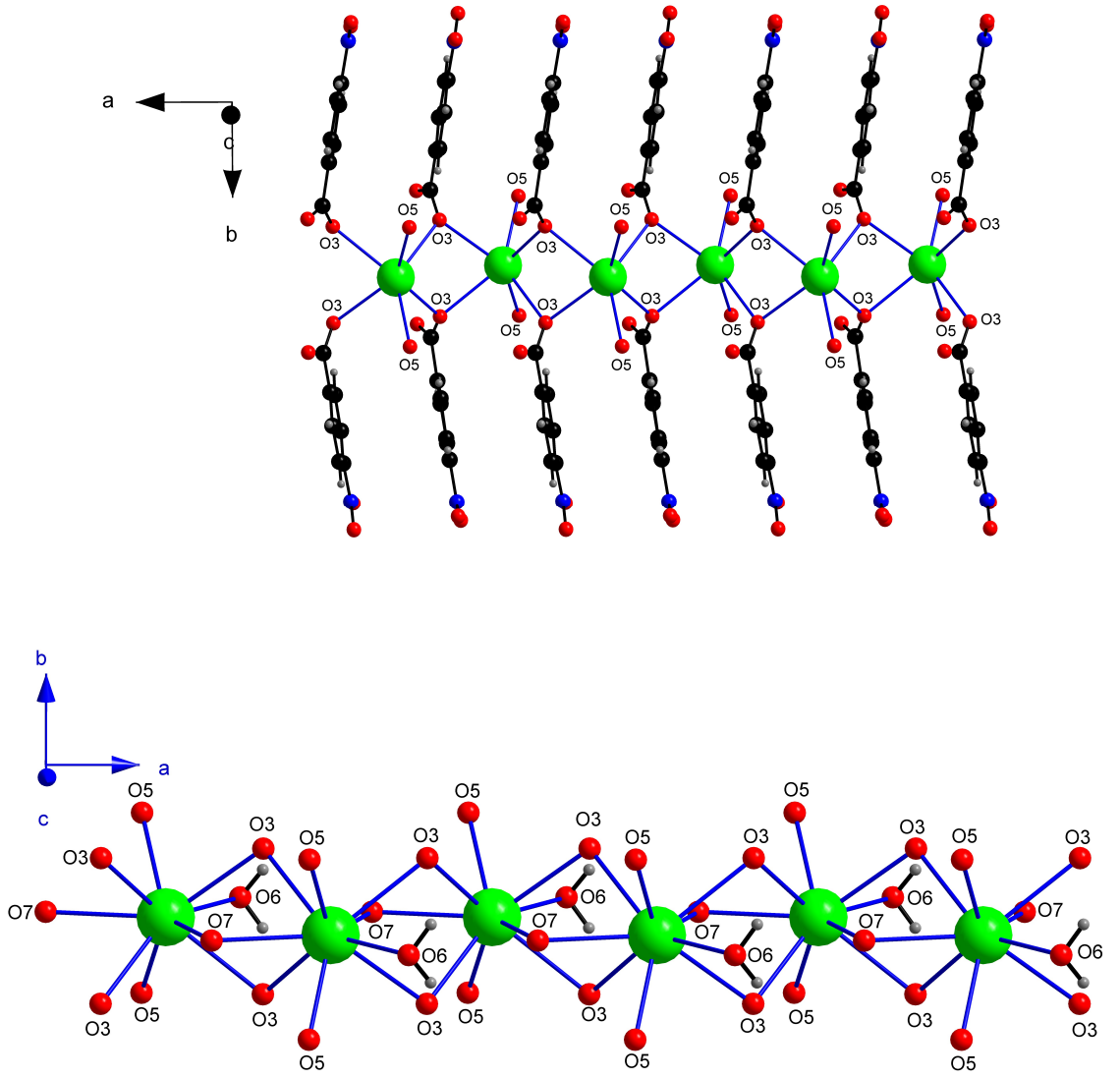

Figure 4–A portion of an infinite chain extending along *a* axis due to the unique μ_2-η^2-bidentate 4-nba ligand in **1**. For clarity, only the O5 of the terminal NMF ligands around each Ba(II) are shown. The bridging and the terminal aqua ligands are not displayed (**Top**). A view of the triple chain polymer showing only the O atoms of the bridging ligands (O3 of 4-nba and O7 of water) and the terminal NMF ligands O5. O6 is terminal water. (**Bottom**).

An analysis of the crystal structure of **1** reveals that the H-atoms H6A and H7A attached to the oxygens of the terminal and bridging water respectively, H1A bonded to N1 of NMF, the H4 atom on C4 of 4-nba and H8 linked to C8 of NMF function as H-donors. The O1 and O4 atoms of 4-nba and O6 of terminal water act as H acceptors resulting in three varieties of H-bonding interactions namely O-H···O, N-H···O and C-H···O respectively [Table S2], which can be classified as intrachain or interchain interactions. The C4-H4···O1 interaction linking the hydrogen atom of a 4-nba ligand of

one chain with the nitro oxygen O1 of an adjacent chain is an interchain interaction and serves to link the parallel polymeric chains [Figure S15].

A comparison of the crystal structure of **1** with that of the precursor pentaaqua compound $[Ba(H_2O)_5(4\text{-nba})_2]$ **1a** reveals certain similarities and quite a few differences. In both the compounds which are one-dimensional, Ba(II) exhibits nine coordination. Unlike the five terminal aqua ligands, a bidentate 4-nba and a symmetrically bridging bidentate 4-nba in **1a**, the title compound **1** contains two types of terminal ligands, namely NMF and water. There are two unique bridging bidentate ligands, namely water (O7) and 4-nba (O3), both of which extend the structure along the same direction resulting in a triple chain. The 4-nba ligand exhibits monoatomic bridging in **1** unlike the symmetrical bridging μ_2-η^1:η^1 mode of 4-nba in **1a** which can account for the differing Ba···Ba separations of 4.2522(3) and 6.750(1) Å respectively in these compounds. In the 1D chain, the $\{BaO_9\}$ polyhedra in **1a** are discretely linked via the C7 atom of the symmetrical bridging 4-nba ligand which joins the adjacent polyhedra [Figure 5].

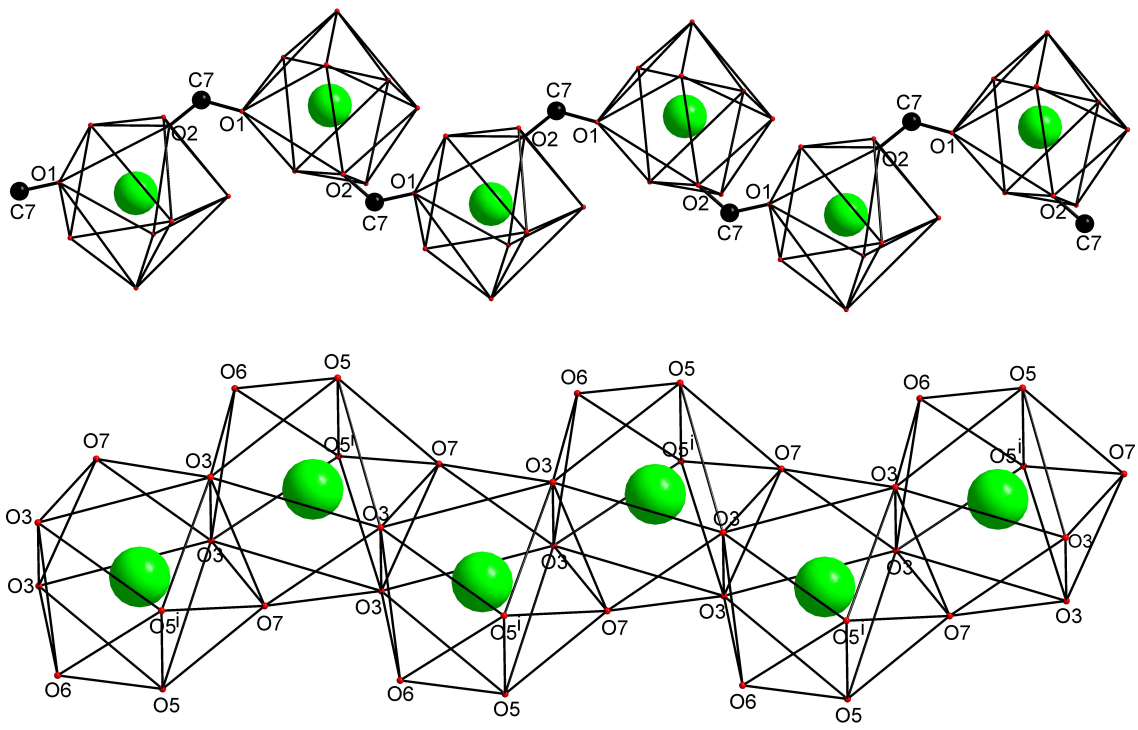

Figure 5 – A portion of the 1D chain showing discrete versus face sharing $\{BaO_9\}$ polyhedra in $[Ba(H_2O)_5(4\text{-nba})_2]$ **1a** (top) and $[Ba(H_2O)_2(NMF)_2(4\text{-nba})_2]$ **1** (bottom). In **1a**, the O1,O2 are the O atoms attached to C7 of the symmetrical bridging 4-nba. In **1**, O5, $O5^i$ and O6 are the terminal ligands

and the O3, O3 and O7 face is shared between adjacent Ba(II) in the chain. Symmetry code: i) x, -y+1/2, z

In contrast, a face shared linking arrangement of the {BaO_9} polyhedra is observed in **1** due to the presence of three common sites (O3, O3 and O7) for each Ba in the chain which carries three terminal ligands namely two NMF (O5, $O5^i$) and a water (O6). Although the Ba in both **1** and **1a** exhibits a distorted monocapped square antiprismatic geometry, the presence of five terminal aqua ligands and a bidentate 4-nba **1a** instead of three terminal ligands in **1** can explain the differing nature of polyhedral linking in the chains of **1a** and **1**.

3.3. Comparative study of barium coordination polymers

The availability of several Ba(II) coordination polymers of based on carboxylate linkers in the literature [9-11, 14,15, 21, 23, 34, 50-81] permits a comaparative study of these compounds, the details of which are given below. For this study a total of fifty eight Ba(II) carboxylates [Table 3] containing examples of one- two and three-dimensional coordination polymers of Ba(II) are taken. It is interesting to note that a majority of the two and three-dimensional compounds excepting entry nos. 23-27 and 52-58 in Table 3 are prepared by hydrothermal or solvothermal methods. All the one dimensional compounds are prepared under ambient conditions. It is interesting to note that all the one-dimensioanl compounds and many two-dimensional compounds contain coordinated water molecules whose number varies from two to five while many three-dimesional compounds have less number of coordinated water per Ba or no water as has been observed in sixteen of the thirty one entries. Although some 2D and 3D compounds have been prepared under ambient conditions, it is to be noted that syntheses performed under hydrothermal conditions result in a lesser degree of hydration as compared to a non hydrothermal synthesis as can be evidenced by the Ba(II) compounds of benzene-1,3,5-tricarboxylic acid (entry nos 36, 41, 42) which are prepared hydrothermally. In contrast the Ba(II) framework (entry no. 58) from the same linker prepared under ambient conditions contains 8 moles of water for three Ba(II) In all these compounds the oxophilic central metal Ba(II) is bonded to O-donor ligands resulting in a {BaOx} (x= 7 to 12) polyhedron. However, three instances (entry nos. 12, 25 and 45) are observed where the Ba(II) is bonded to a single N in addition to oxygen and one example where Ba is bonded to two N (entry no. 21). In these compounds the reported Ba-N

distances are 2.911(5), 3.047(4), 2.906(7) and 2.9662(16) Å respectively and are longer compared to the Ba-O distances. Based on the reported Ba-O distances which range from 2.625(16) (entry no. 31) to 3.189(7) Å (entry no. 36) in these compounds, it can be inferred that Ba-O bond lengths scatter in the range 2.6 to 3.2 Å. In view of a wide range of Ba-O bond lengths and O-Ba-O bond angles, in general the {BaOx} poyhedra are distorted from regular geometries.

Out of the fifty eight entries in Table 3, twenty compounds contain more than one unique Ba in the crystal structure and thus a total of 96 Ba(II) sites are observed. A survey of the coordination numbers of barium reveals the structural flexibility of Ba(II) to exhibit coordination numbers ranging from seven to twelve. Of these, the most preferred coordination number is nine which is observed in forty seven Ba(II) sites including the title compound. The coordination number eight is observed in twenty nine Ba(II) centres while more than a dozen examples of $\{BaO_{10}\}$ polyhedron are observed. A majority (forty six out of fifty eight) of the compounds in Table 3 crystallize in centrosymmetric space groups.

The Ba···Ba separations in these compounds are determined by a combination of many factors, which include the electronic and steric requirements of the central metal, the denticity, flexibility, bridging behavior and H-bonding characteristics of the ligand. Although the 2D and 3D compounds can in principle have more than one separation, only the shortest Ba···Ba separation is listed in Table 3. It is noteworthy to mention that the Ba···Ba separations vary from 3.8798(8) Å in the two dimensional (2D) coordination polymer (entry No. 11) derived from 4,4′-sulfobis(benzoic acid) to 7·626(19) Å in the 2D Ba(II) polymer (entry No. 22) derived from 3-[(3-carboxy-phenoxy)phthalic acid]. The Ba···Ba separation of 3.8798(8) Å (entry No. 11) is shorter than the sum of the van der Waals radii (4·28 Å) indicating weak metal–metal interactions. Several more including the title compound, belong to this category. The Ba···Ba separations range between 4.0877(7) to 4.937(7) Å in all the 3D polymers while these values span a broader range between 3.8798(8) to 7.626(19) Å in both 1D and 2D compounds.

A comparison of the Ba···Ba distances in compounds **1** and **1a** where the same 4-nba ligand bridges the metal centers illustrates that when one of the carboxylate oxygen binds to a minimum of two Ba(II) ions (monoatomic bridging) as in **1**, the Ba···Ba distances are shorter which can probably be explained due to the geometrical constraints. When the carboxylate ligand exhibits symmetrical bridging (μ_2-η^1:η^1) binding mode, the separations tend to be longer. In the 3D polymers and also in many other compounds it is noted that the carboxylate group exhibits multidentate (tri or tetradentate) binding wherein at least one of the carboxylate oxygen is linked to a minimum of two metal ions, which can explain the shorter separations. This is demonstrated by the nonanuclear compound $[Ba_9(CH_3COO)_{14}(ClO_4)_4]$ wherein the acetates exhibit three different bridging binding modes viz. μ_5-η^3:η^3, μ_4-η^2:η^2 and μ_3-η^2:η^2 respectively resulting in the binding of a minimum of two metals to each carboxylate oxygen. The observed Ba···Ba separation is 4.27 Å.

Longer separations between the central metals can occur in a multicarboxylate ligand wherein each carboxylate exhibits monodentate binding as observed in the 2D compound $[Ba(H_2O)_5(H_2PMA)]$ (H_4PMA is pyromellitic acid). The dianion of pyromellitic acid functions as a tetradentate bridging ligand (μ_4-η^1:η^1:η^1:η^1) binding to four Ba(II) ions [Figure S16] and each Ba(II) is bonded to five terminal aqua ligands. This results in the longer Ba···Ba separation of 6.65 Å and each (H_2PMA) ligand is linked to four $\{BaO_9\}$ polyhedra in this compound leading to a discrete linking of the $\{BaO_9\}$ polyhedra. A similar argument holds good for the long Ba···Ba separation of 6.765(3) Å in the 2D compound $[Ba(H_2IDC)_2(H_2O)_4]\cdot 2H_2O$ (entry no 21) where each of the –COO moiety binds to a single Ba. In the three-dimensional barium terephthalate compound each of the carboxylate oxygen functions as a monoatomic bridge and thus exhibits μ_7-octadentate binding mode [Figure S17]. In this anhydrous compound, the Ba···Ba separation is very short at 4.123 Å.

4. Conclusions

In this work, we have shown that coordination polymers can be synthesized under ambient conditions by a proper choice of the reagents. The one-dimensional barium coordination polymer described in this report is a new addition to the growing list of structurally characterized alkaline-earth metal

coordination polymers based on the 4-nitrobenzoic acid linker, containing terminal amide ligands. The shorter metal-amide oxygen distances in **1** indicate that amides can be considered as useful ancillary ligands for the synthesis of new alkaline-earth coordination polymers. A comparative study of fifty eight barium coordination polymers reveals a rich and variable structural chemistry of Ba(II) based on bridging carboxylate ligands.

Supplementary Material

Crystallographic data in CIF format for the structure of $[Ba(H_2O)_2(NMF)_2(4\text{-nba})_2]$ (**1**) reported in this paper have been deposited with the Cambridge Crystallographic Data Centre as supplementary publication no. CCDC 1908263. Copies of the data can be obtained, free of charge, on application to CCDC, 12 Union Road, Cambridge CB2 1 EZ, UK. (fax: +44-(0)1223-336033 or email: deposit@ccdc.cam.ac.uk). Additional figures and Tables related to the crystal structure, and Infrared spectra, Raman spectra, P-XRD, UV-visible spectra, Photoluminescence spectra, TG-DTA (Fig. S1 to Fig. S17; Table S1 & Table S2) are available as 'Supplementary Data' for this article and can be found in the online version.

Acknowledgements

Authors thank the Sophisticated Analytical Instrument Facility (SAIF), Indian Institute of Technology (IIT) Madras for single crystal X-ray analysis of **1** reported in this paper. The authors thank one of the reviewers for useful suggestions.

Funding

BRS thanks the University Grants Commission (UGC), New Delhi for financial support to the School of Chemical Sciences (formerly Department of Chemistry), at the level of DSA-I under the Special Assistance Program (SAP) vide letter F.No. 540/14/DSA-I/2015/(SAP-I). PHB is a recipient of the BSR Fellowship (Supernumerary fellowship for "Single Girl Child") by UGC, New Delhi *vide* letter F.No.25-1/2014-15(BSR)/7-69/2007(BSR).

References

1. K.M Fromm. *Coord. Chem. Rev.*, **252,** 856-885 (2008).
2. D. Banerjee, J.B Parise, *Cryst. Growth. Des.*, **11**, 4704-4720 (2011).
3. A. Chanthapally, H.S Quah, J.J. Vittal, *Cryst. Growth. Des.*, **14**, 2605-2613 (2014).
4. D-L. Yang, X. Zhang, Y-G. Yao, J. Zhang, *CrystEngComm.*, **16**, 8047-8057(2014).
5. D.L. Reger, A.P. Leitner, M.D. Smith, *Cryst. Growth. Des.*, **16**, 527-536 (2016).
6. Y. Ling, D. Bai, Y. Feng, Y. He, *J. Solid State Chem.*, **242**, 47-54 (2016).
7. D. Chen, D. Jing, Q. Zhang, X. Xue, S. Gou, H. Li, F. Nie, *Chem. Asian J.*, **12**, 3141-3149 (2017).
8. N. Yuan, M. Zhang, H. Cai, Z. Liu, R. Zhao, *Inorg. Chem. Commun.*, **101**, 130-134 (2019).
9. M.L. Foo, S. Horike, S. Kitagawa, *Inorg. Chem.*, **50**, 11853-11855 (2011).
10. M.L. Foo, S. Horike, Y. Inubushi, S. Kitagawa, *Angew. Chem. Int. Ed.*, **51**, 6107-6111 (2012).
11. M.L. Foo, S. Horike, J. Duan, W. Chen, S. Kitagawa, *Cryst. Growth. Des.*, **13**, 2965-2972 (2013).
12. K.S. Asha, M. Makkitaya, A. Sirohi, L. Yadav, G. Sheet, S. Mandal, *Cryst Eng Comm.*, **18**, 1046-1053 (2016).
13. G.W. Yang, Y.T. Zhang, Q. Wu, M.J. Cao, W. Jiao, Q.Y. Yue, Q.Y. Li, *Inorganica Chimica Acta.*, **450**, 364-371 (2016).
14. D. Smets, M. Sobieraya, U. Ruschewitz, IUCrData (2016).1 x161409 (2016).
15. X. Zhang, Y-Y. Huang, M-J. Zhang, J. Zhang, Y.G. Yao, *Cryst. Growth Des.*, **12**, 3231-3238 (2012).
16. X. Wang, L.K. San, H. Nguyen, N.M. Shafer, M.T. Hernandez , Z. Chen, *J. Coord. Chem*, **66**, 826-835 (2013).
17. M-L. Chen,Y-H. Hou,W-S. Xia, Z-H. Zhou, *J. Coord. Chem*., **66**, 1906-1915 (2013).
18. N. Marino, R. Bruno, D. Armentano, G. D. Munno, *J. Coord. Chem.*, **71**, 828-844 (2018)
19. C. Dey, T. Kundu, B.P. Biswal, A. Mallick and R. Banerjee, *Acta Crystallogr*., **B70**, 3-10 (2014).
20. M.B. Cingi, A.M.M. Lanfredi, A. Tiripicchio, M.T. Camellini, *Acta Crystallogr.*, **B34,** 774-778 (1978).
21. R. Murugavel, K. Baheti, G. Anantharaman, *Inorg. Chem.*, **40**, 6870-6878 (2001).
22. B.R. Srinivasan, S.Y. Shetgaonkar, P. Raghavaiah, *Polyhedron*, **28**, 2879-2886 (2009).

23. B.R. Srinivasan, S.Y. Shetgaonkar, P. Raghavaiah, *Indian. J. Chem*., **51A,** 1064-1072 (2012).

24. R. Murugavel, S. Banerjee, *Inorg. Chem. Commun.*, **6,** 810-814 (2003).

25. R. Murugavel, R. Korah, *Inorg. Chem.*, **46**, 11048-11062 (2007).

26. B.R. Srinivasan, S.Y. Shetgaonkar, *J. Coord Chem*., **63,** 3403-3412 (2010).

27. K.T. Dhavskar, P.H. Bhargao, B.R. Srinivasan, *J Chem Sci.*, **128**, 421-428 (2016).

28. W. Starosta, J. Leciejewicz, T. Premkumar, S. Govindarajan, *J. Coord.Chem*., **60**, 313-318 (2016).

29. N.T. Pour, A. Khalighi, M. Yousefi, V. Amani, *Synthesis and Reactivity in Inorganic, Metal-Organic, and Nano-Metal Chemistry*, **45**, 1427-1433 (2005).

30. T-T Li, S-L. Cai, R-H. Zeng, S-R. Zheng, *Inorg. Chem. Commun*, **48**, 40-43 (2014).

31. W-Z. Zhang, T-Y. Lv, D-Z. Wei, R. Xu, G. Xiong, Y-Q. Wang, E-J. Gao, Y-G. Suna, *Inorg. Chem. Commun.*, **14**, 1245-1249 (2011).

32. S. Halake, K.M. Ok, *J. Solid State Chem*, **231,** 132-137 (2015).

33. N.R. Kelly, S. Goetz, S.R. Batten, P.E. Kruger, *CrystEngComm.*, **10,** 68-78 (2008).

34. X. Chen, S. He, F. Chen, Y. Feng, *CrystEngComm.*, **16,** 8706-8709 (2014).

35. S.B. Ge,C. Liu, G. Wu, *Synthesis and Reactivity in Inorganic, Metal-Organic, and Nano-Metal Chemistry*., **45**, 122-126 (2015).

36. G. Scholz, A. Abdulkader, E. Kemnitz, *Z. Anorg. Allg. Chem.*, **640**, 317-324 (2014).

37. A-A Al-Terkawi, G. Scholz, F. Emmerling, E. Kemnitz, *Solid State Sci.*, **79**, 99-108 (2018).
38. F. Moghzi, J. Soleimannejad, *Ultrason. Sonochem.*, **42,** 193-200 (2018).

39. A. Drzewiecka-Antonik, A. E. Koziol, P. Rejmak, K. Lawniczak-Jablonska, L. Nittler, T. Lis, *Polyhedron.*, **132**, 1-11 (2017).

40. B.R. Srinivasan, S.Y. Shetgaonkar, P. Raghavaiah, *J. Chem. Sci.*, **120**, 249-257 (2008).

41. B.R. Srinivasan, K.T. Dhavskar, C. Näther, *J. Chem. Sci.* **128**, 1765-1774 (2016).

42. B.R. Srinivasan, S.Y. Shetgaonkar, C. Näther, *Z. Anorg. Allg. Chem.*, **637**, 130-136 (2011).

43. B.R. Srinivasan, S.Y. Shetgaonkar, N.N. Ghosh, *J. Coord. Chem*., **64**, 1113-1124 (2011).

44. B.R. Srinivasan, J.V. Sawant, S.C. Sawant, P. Raghavaiah, *J. Chem. Sci*., **119,** 593-601 (2007).

45. B.R. Srinivasan, J.V. Sawant, C. Näther, W. Bensch, *J. Chem. Sci*., **119**, 243-252 (2007).

46. B.R. Srinivasan, J.V. Sawant, P. Raghavaiah, *Indian. J. Chem.*, **45A**, 2392-2399 (2006).

47. B.R. Srinivasan, P. Raghavaiah, J.V. Sawant, *Acta Crystallogr.*, **E63**, 2251-2252 (2007).

48. B.R. Srinivasan, K.T. Dhavskar, *Indian. J. Chem*. Section A, **56**, 387-393 (2017).

49. G. M. Sheldrick, *Acta. Crystallogr.*, **C71**, 3--8 (2015).

50. A. Briceno, J.M. Delgado, G.D. Delgado, *Acta Crystallogr.*, **E58**, m602-605 (2002).

51. S. M. F. Lo, S.S.Y Chui, I.D. Williams, *Acta Crystallogr.*, **C54**, 1846-1848 (1998).

52. M. Odabasoglu, O. Buyukgungor, *Acta Crystallogr.*, **E62**, m402-404 (2006).

53. R.L. Garzon, M.D.L. Leon, J.N. Low, C. Glidewell, *Acta Crystallogr.,* **C61**, m224-227 (2005).

54. M.L.G. Salido, P.A. Mascaros, R.L. Garzon, M.D.G. Valero, J.N. Low, J.F. Gallagher, C. Glidewell, *Acta Crystallogr.*, **B60**, 46-64 (2004).

55. R. Murugavel, V.V. Karambelkar, G. Anantharaman, M.G. Walawalkar, *Inorg. Chem.*, **39**, 1381-1390 (2000).

56. S. Djehni, F. Balegroune, A. Guehria-Laidoudi, S. Dahaoui, C. Lecomte, *Acta Crystallogr.*, **C63**, m91-93 (2007).

57. S.H. Dale, M.R.J. Elsegood, S. Kainth, *Acta Crystallogr.* **C59** m505-508 (2003).

58. X. Zhang, S. Gao, L.H. Huo, H. Zhao, *Acta Crystallogr.,* **E61**, m2488-2490 (2005).

59. B.H. Lee, C.H. Kim, S.G. Lee, *Acta Crystallogr.,* **C59**, m196-198 (2003).

60. D. Guo, B-G. Zhang, C-Y. Duan, K-L. Pang, Q-J. Meng, *J. Chem. Soc. Dalton Trans.*, **0** 3783-3784 (2002).

61. S. Gao, J.W. Liu, L.H. Huo, H. Zhao, *Acta Crystallogr*., **C61**, m348-350 (2005).

62. K-Li. Cao, Y. Xia, G-X. Wang , Y-L. Feng, *Inorg. Chem. Commun*, **53**, 42–45 (2015).

63. W-L. Chen, W-X. Chen, G-L. Zhuang, J. Zheng, L. Tan, X. Zhong, J-G. Wang, *Cryst. Eng. Comm*, **15**, 5545–5551 (2013).

64. X-Y. Dong, X-P. Hu, H-C. Yao, S-Q. Zang, H-W. Hou, T. C.W. Mak, *Inorg. Chem.* **53**, 12050−12057 (2014).

65. A. Douvali, G.S. Papaefstathiou, M.P. Gullo, A. Barbieri, A.C. Tsipis, C.D. Malliakas, M.G. Kanatzidis, I. Papadas, G.S. Armatas, A.G. Hatzidimitriou, T. Lazarides, M.J. Manos, *Inorg. Chem.,* **54**, 5813-5826 (2015).

66. S. Du, C. Ji, X. Xin, M. Zhuang, X. Yu, J. Lu, Y. Lu, D. Sun, *J. Mol. Struct.* **1130**, 565-572 (2017).

67. M. Kang, T. Liu, X. Wang, D. Luo, R. Li, Z. Lin, *Inorg. Chem. Commun*, **44,** 155–158 (2014).

68. M. K. Kim, K. M. Ok , *CrystEngComm.*, **13**, 4599–4603 (2011).

69. T. Kundu, S.C. Sahoo, R. Banerjee, *Chem. Commun.*, **48**, 4998–5000 (2012).

70. F. Liu, Y. Xu, L. Zhao, L-L Zhang, W. Guo, R. Wang, D. Sun, *J. Mater. Chem. A*, **3**, 21545-21552 (2015).

71. P.C. Rao, K.S. Asha, S. Mandal, *CrystEngComm.,* **16**, 9320-9325 (2014).

72. D. Saha, T. Maity, R. Sen, S. Koner, *Polyhedron,* **43**, 63–70 (2012).

73. G.D. Tarlas, A.D. Katsenis, G.S. Papaefstathiou, *Eur. J. Inorg. Chem.*, **2018**, 4458-4464 (2018).

74. P. Vishnoi, D. Kaleeswaran, A.Ch. Kalita, R. Murugavel, *CrystEngComm*., **18**, 9130-9138 (2016).

75. R. Wang, X. Liu, A. Huang, W. Wang, Z. Xiao, L. Zhang, F. Dai, D. Sun, *Inorg. Chem.*, **55**, 1782-1787 (2016).

76. D. Xiao, H. Chen, D. Sun, J. He, S. Yan, J. Yang, X. Wang, R. Yuana, E. Wang, *CrystEngComm*., **14**, 2849-2858 (2012).

77. R-P. Ye, J-X. Yang, X. Zhang, Y-G. Yao, *Z. Anorg. Allg. Chem.*, **642**, 60-65 (2016).

78. U.S.S Mol, R.M. Nair, R. Drisya, P.R.S. Chandran, M.R. Sudarsanakumar, S.W. Ng, M.R.P. Kurup, *Main Group Met. Chem.*, **39**, 157–165 (2016).

79. D. Briones, P. Leo, J. Cepeda, G. Orcajo, G. Calleja, R. Sanz, A. Rodríguez-Diéguez, F. Martínez, *CrystEngComm*., **20**, 4793-4803 (2018).

80. M.J. Plater, A.J. Roberts, J. Marr, E.E. Lachowski, R.A. Howie, *J. Chem. Soc. Dalton Trans.*, 797-802 (1998).

81. Y-C. Gao, Q-H. Liu, F-W. Zhang, G. Li ,W-Y. Wang, H-J. Lu , *Polyhedron*, **30**, 1-8 (2011).

Table 3 – Structural features of some barium coordination polymers.

No	Compound	S.G	Ba···Ba (Å) separation*	C.N	C.S	Ba-O distances (Å)	Ref
One-dimensional (1D) [§]							
1	$[Ba(Hbpdc)_2(H_2O)_2]$	$P2_1/n$	4.1386(17)	9	$\{BaO_9\}$	2.6922(19)-2.9144(15)	[50]
2	$[Ba(H_2O)_2(NMF)_2(4\text{-nba})_2]$	*Pnma*	4.2522(3)	9	$\{BaO_9\}$	2.749(3)-2.953(4)	This work
3	$[Ba(C_7H_5O_2S)_2(H_2O)_4]$	*Pnma*	4·3355(13)	9	$\{BaO_9\}$	2.768(4)-2.946(3)	[59]
4	$[Ba(C_8H_5O_3)_2(H_2O)_2]$	C_2/c	4·4336(3)	8	$\{BaO_8\}$	2.6599(19)- 2.905(2)	[53]
5	$[Ba(PY\text{-}met)_2(H_2O)_4]\cdot 3H_2O$	$P4_3$	4·4451(2)	10	$\{BaO_{10}\}$	2.747(3)-2.915(3)	[55]
6	$[Ba(H_2O)_3(2\text{-nba})_2]_2$	$P\bar{1}$	4·5406(15)	9	$\{BaO_9\}$	2.703(2)-2.906(2)	[40]
7	$[Ba(C_{10}H_{12}N_5O_6)_2(H_2O)_6]$	$P2_1$	6·575(0)	9	$\{BaO_9\}$	2.715(3)-2.939(4)	[54]
8	$[Ba(H_2O)_5(4\text{-nba})_2]$	$P2_1/c$	6·750(1)	9	$\{BaO_9\}$	2.7616(18)-2.8981(18)	[44]
9	$[Ba(PY\text{-glycinato})_2(H_2O)_5]\cdot H_2O$	$P2_1/c$	6·916(1)	9	$\{BaO_9\}$	2.656(8)-2.866(8)	[55]
10	$[Ba(PY\text{-serinato})_2(H_2O)_4]\cdot 3H_2O$	*P*1	7·139(0)	10	$\{BaO_{10}\}$	2.695(3)-3.238(4)	[55]
Two-dimensional (2D) [$]							
11	[Ba-SBBA]	$P\bar{1}$	3.8798(8)	9, 10[#]	$\{BaO_9\}$ $\{BaO_{10}\}$	2.706(4)-3.019(5)	[69]
12	$[Ba_2L_2(H_2O)_3]\cdot 5.5H_2O$	$P2_1/c$	4.2655(5)	9, 9[#]	$\{BaO_8N\}$ $\{BaO_9\}$	2.677(4)-3.029(5)	[62]
13	$[Ba_5(OBDC)_4(H_2O)_2(NO_3)_2]$	$P\bar{1}$	4.5443(7)	8, 8, 8[#]	$\{BaO_8\}$	2.676(6)-3.082(6)	[15]
14	$[Ba(\mu_2\text{-}OH_2)(sdba)(H_2O)_3]\cdot 0.25(bim)\cdot H_2O$	$P\bar{1}$	4.6904(2)	9	$\{BaO_9\}$	2.7136(15)-2.8873(16)	[76]
15	$[Ba(\mu_2\text{-}OH_2)(sdba)(H_2O)_3]\cdot 0.5(C_6H_6)\cdot H_2O$	$P\bar{1}$	4.7101(3)	9	$\{BaO_9\}$	2.717(2)-2.906(2)	[76]
16	$[Ba(\mu_2\text{-}OH_2)(sdba)(H_2O)_3]\cdot 0.5(bpy)\cdot H_2O$	$P\bar{1}$	4.7108(4)	9	$\{BaO_9\}$	2.7241(18)-2.8943(18)	[76]
17	$[Ba(\mu_2\text{-}OH_2)(sdba)(H_2O)_3]$ $0.5(dfb)\cdot 0.25H_2O$	$P\bar{1}$	4.7127(17)	9	$\{BaO_9\}$	2.713(6)-2.899(6)	[76]
18	$[Ba(\mu_2\text{-}OH_2)(sdba)(H_2O)_3]\cdot 0.5(tolu)\cdot H_2O$	$P\bar{1}$	4.7153(4)	9	$\{BaO_9\}$	2.7140(17)-2.9112(18)	[76]
19	$[Ba(\mu_2\text{-}OH_2)(sdba)(H_2O)_3]\cdot 0.5H_2O$	$P\bar{1}$	4.7192(16)	9	$\{BaO_9\}$	2.704(4)-2.917(4)	[76]
20	$[Ba(\mu_2\text{-}OH_2)(sdba)(H_2O)_3]\cdot 3.5H_2O$	$P\bar{1}$	4.7456(14)	9	$\{BaO_9\}$	2.724(4)-2.894(4)	[76]
21	$[Ba(H_2IDC)_2(H_2O)_4]\cdot 2H_2O$	C_2/c	6·765(3)	10	$\{BaN_2O_8\}$	2.8501(15)-2.9104(15)	[58]
22	$[Ba(HL)(H_2O)_3]\cdot nH_2O$	$P\bar{1}$	4.579	9	$\{BaO_9\}$	2.705(3)-2.926(2)	[77]
23	$[Ba_5(CH_3COO)_2(C_8H_4O_4)_4]$[ǂ]	$P\bar{1}$	4.1893(4)	8, 9, 12[#]	$\{BaO_8\}$ $\{BaO_9\}$ $\{BaO_{12}\}$	2.706(2)-3.091(3)	[78]
24	$[Ba(H_2PMA)(H_2O)_5]$[□]	$P2_1/m$	6·65	9	$\{BaO_9\}$	2.6742(19)-2.8690(13)	[57]

25	$[Ba(2\text{-}aba)_2(H_2O)_2]^{\S}$	*Pbcn*	4·32	9	$\{BaO_8N\}$	2.671(3)-3.011(4)	[56]
26	$[Ba(C_5H_4O_4)_2(H_2O)_4]^{\S}$	$P2_1/n$	4·595(4)	9	$\{BaO_9\}$	2.683(3)-2.967(4)	[51]
27	$[Ba(PY\text{-}glycilglycinato)_2(H_2O)_2]^{\S}$	C_2/c	7·467	8	$\{BaO_8\}$	2.762(2)-2.808(3)	[55]
Three-dimensional (3D)$^{\$}$							
28	$[Ba(NH_2\text{-}bdc)(DMF)]$	$P3_1$	4.0877(7)	8	$\{BaO_8\}$	2.653(6)-2.933(6)	[79]
29	$[Ba_9(TCMTB)_4(NO_3)_6(DMAc)_{14}]$	$P\bar{1}$	4.1254(8)	8, 8, 8, 8, 9, 9, 9, 9, 9$^{\#}$	$\{BaO_8\}$ $\{BaO_9\}$	2.628(4)-2.982(5)	[74]
30	[Ba(pdc)]	*Pbca*	4.161(0)	7	$\{BaO_7\}$	2.66(3)-2.93(14)	[72]
31	$[Ba_5(ADDA)_5(EtOH)_2(H_2O)_3]\cdot 5DMF$	$P\bar{1}$	4.2231(17)	7, 8, 9, 10$^{\#}$	$\{BaO_7\}$ $\{BaO_8\}$ $\{BaO_9\}$ $\{BaO_{10}\}$	2.625(16)-3.154(16)	[75]
32	$[Ba_2(dbtec)(H_2O)_2]$	*Acam*	4.254	10, 10$^{\#}$	$\{BaO_{10}\}$	2.760-3.027	[66]
33	[Ba(HBTB)(DMF)]·DMF	$Pna2_1$	4.2601(6)	9	$\{BaO_9\}$	2.754(9)-2.946(5)	[9]
34	$[Ba_2(H_2btec)\cdot H_2O]\cdot 0.5H_2O$	*C2/c*	4.2643(3)	9,10$^{\#}$	$\{BaO_9\}$ $\{BaO_{10}\}$	2.656-3.058	[66]
35	$[Ba_2(BTTC)(H_2O)_2]$	$Pn2_1a$	4.265(0)	8, 9$^{\#}$	$\{BaO_8\}$ $\{BaO_9\}$	2.671(3)-3.003(3)	[11]
36	$[Ba_2TMA(NO_3)(DMF)]\cdot DMF$	$P\bar{6}2c$	4.281(0)	8, 9$^{\#}$	$\{BaO_8\}$ $\{BaO_9\}$	2.703(4)-3.189(7)	[10]
37	$[Ba_3(BPTC)_2(NMF)_5]\cdot 2NMF$	$I\bar{4}2d$,	4.319(0)	8, 9$^{\#}$	$\{BaO_8\}$ $\{BaO_9\}$	2.678(8)-3.097(16)	[11]
38	[Ba(ndc)(DMF)]	$P2_12_12_1$	4.3361(7)	7	$\{BaO_7\}$	2.642(4)-2.814(3)	[67]
39	$[Ba_5(L_3)_3(H_2O)_6]\cdot 25H_2O\cdot 10DMF\cdot 2Me_2NH_2^+$	*P6/m*	4.337	9, 10$^{\#}$	$\{BaO_9\}$ $\{BaO_{10}\}$	2.775(4)-2.971(4)	[34]
40	$[Ba(H_2L_4)(H_2O)]$	*C2221*	4.401	10	$\{BaO_{10}\}$	2.710(3)-3.010(3)	[73]
41	$[Ba(HBTC)(H_2O)_2]\cdot 0.5H_2O$	$P\bar{1}$	4.464	9	$\{BaO_9\}$	2.722(6)-2.877(6)	[80]
42	$[Ba_3(BTC)_2(H_2O)_4]$	$Pna2_1$	4.467	7, 8, 9$^{\#}$	$\{BaO_7\}$ $\{BaO_8\}$ $\{BaO_9\}$	2.661(11)-2.968(15)	[15]
43	$[Ba(H_2MIDC)_2]$	$P2_1/n$	4.5435(5)	9	$\{BaO_9\}$	2.720(3)-3.047(2)	[81]
44	[Ba(BPDC)]	*C2/m*	4.5754(9)	8	$\{BaO_8\}$	2.6895(15)-2.8942(15)	[11]
45	$[Ba(2,6\text{-}NC_5H_3(CO_2)_2)]$	*C2/c*	4.727(39)	7	$\{BaO_6N\}$	2.698(4)-2.803(5)	[68]
46	$[Ba(1,3\text{-}BDOA)(H_2O)_2]$	$P2_1/c$	4·755(3)	10	$\{BaO_{10}\}$	2.736(2)-3.173(3)	[61]
47	$[Ba(H_2L^{OMe})_{0.5}]4H_2O$	*C2/c*	4.808(0)	8	$\{BaO_8\}$	2.707(5)-2.960(5)	[70]
48	$[Ba(H_2L^{OMe})_{0.5}(H_2O)]\cdot 4H_2O$	*C2/c*	4.818(6)	9	$\{BaO_9\}$	2.699(10)-2.888(10)	[70]

49	[Ba(H_2dhtp)(DMAc)]	*C2/c*	4.891(0)	9	{BaO_9}	2.636(8)-2.9413(18)	[65]
50	[$Ba_2(H_2L^{OMe})_2$(NMP)]·NMP	*P*$\bar{1}$	4.937(7)	8, 8#	{BaO_8}	2.756(5)-2.975(6)	[70]
51	[$Ba_6(BPTC)_3(H_2O)_6$]·$11H_2O$	$P2_1/c$	4.497(1)	7, 8, 9, 9, 9, 9#	{BaO_7} {BaO_8} {BaO_9}	2.650-3.056	[64]
52	[Ba(tfBDC)(DMF)(EtOH)]¤	$P2_1/c$	4.4999(3)	8, 8#	{BaO_8}	2.603(17)-2.886(3)	[14]
53	[Ba(PODC)$(H_2O)_2$]◊	*C2/c*	4.642	10	{BaO_{10}}	2.7790(18)-3.118(2)	[63]
54	[$Ba_2O_3(OBA)_2$]◊	$Pca2_1$	4.500(1)	8, 9#	{BaO_8} {BaO_9}	2.706(5)-2.976(5)	[71]
55	[Ba($C_6H_4(COO)_2$)]□	*Pbca*	4·123	8	{BaO_8}	2.711(3)-2.944(3)	[52]
56	[Ba_2(DTBB)$_2(H_2O)_2$]·0·$5H_2O$]§	*Pccn*	4·069(2)	9, 8, 8#	{BaO_8} {BaO_9}	2.627(1)-3.00(5)	[21]
57	[$Ba_9(CH_3COO)_{14}(ClO_4)_4$]§	C_2/m	4·27	8, 9, 9#	{BaO_8} {BaO_9}	2.657(2)-3.045(3)	[60]
58	[Ba_3(BTC)$_2(H_2O)_8$]·$2H_2O$§	$P2_1/c$	4.570	8, 10#	{BaO_8} {BaO_{10}}	2.6548(18)-3.013(2)	[23]

Abbreviations used: S.G = Space Group, CN = coordination number; *For 2D and 3D polymers only the shortest Ba···Ba separation is given. C.S = Coordination Sphere; # two or more unique Ba(II) ions; $ Most of the compounds are prepared under Hydrothermal / Solvothermal conditions; § = Slow Evaporation; ¤ = Diffusion method; ⋕ = Gel technique; ◊ = Sonochemical method; □ = Layer Diffusion method; Hbpdc = 2′-carboxybiphenyl-2-carboxylate; NMF = N-methylformamide, 4-nba = 4-nitrobenzoate; ($C_7H_5O_2S$) = thiosalicylate; ($C_8H_5O_3$) = 2-formylbenzoate; PY = N-(6-amino-3,4-dihydro-3-methyl-5-nitroso-4-oxopyrimidin-2-yl); met = monoanion of methionine; 2-nba = 2-nitrobenzoate; ($C_{10}H_{12}N_5O_6$) = N-(4-amino-1,6-dihydro-1-methyl-5-nitroso-6-oxopyrimidin-2-yl)-(S)-glutamato; (SBBA) = 4,4'-sulfobisbenzoic acid; H_4L_2 = 5-(4-(2,6-di(pyridin-4-yl)pyridin-4-yl)phenoxy) isophthalic acid; ($C_8H_4O_4$/H_2OBDC) = phthalic acid; (sdba) = 4,4'-sulfonyldibenzoate; (bim) = 1,4-bis(imidazol-1-yl)butane; C_6H_6 = benzene; (bpy) = 2,2'-bipyridine; (dfb) = 1,3Difluoro-benzene; (tolu) = toluene; (H_2IDC) = 1H-imidazole-4,5-dicarboxylato monoanion; (H_3L) = 3-[(3-carboxy-phenoxy)phthalic acid]; (CH_3COO) = acetate; (H_4PMA) = pyromellitic acid; (2-aba) = 2-aminobenzoate; $C_5H_4O_4$ = mesaconate anion; NH_2-bdc = 2-amino-1,4-benzenedicarboxylate; (H_3TCMTB) = 2,4,6-tris[(4'-carboxyphenoxy)methyl]-1,3,5-trimethylbenzene; DMAc = N, N-dimethylacetamide; (H_2pdc) = pyridine-2,5-dicarboxylic acid); (H_2ADDA) = 3,3′-(anthracene-9,10-diyl)diacrylic acid; EtOH=Ethanol; DMF = N,N-Dimethyl formamide; H_4dbtec = 3,6-dibromobenzene-1,2,4,5-tetracarboxylic acid; H_3BTB = Benzene-1,3,5-trisbenzoic Acid; H_4btec = benzene-1,2,4,5-tetracarboxylic acid; (H_4BTTC) = biphenyl-3,3′,5,5′-tetracarboxylic acid; H_3BTC/H_3TMA= 1,3,5-benzenetricarboxylic acid or trimesic acid; BPTC= (2,2′,6,6′-tetracarboxybiphenyl); ndc = 1,4-naphthalenedicarboxylate; (H_4L_3) = biphenyl-3,3′,5,5′-tetra-(phenyl-4-carboxylic acid); (H_4L_4) = 4-(carboxyformamido)-2-hydroxybenzoic acid; (H_3MIDC) = 2-methyl-1*H*-imidazole-4,5-dicarboxylic acid; (H_2BPDC) = 4,4′-biphenyldicarboxylic acid; [2,6-$NC_5H_3(CO_2H)_2$] = 2,6-pyridinedicarboxylic acid; (1,3-BDOA) = m-phenylenedioxyacetate; (H_4**L**^{OMe})= 5,5'-(2,3,6,7-tetramethoxy-anthracene-9,10-diyl)diisophthalic acid; H_4dhtp = 2,5-dihydroxy-terepthalic acid; NMP = N-Methyl-2-pyrrolidone, (tfBDC) = tetrafluoroterephthalate; H_2PODC = 2,5-piperazinedione-1,4-diacetic acid; HOBA=4,4'-oxy-bis(benzoic acid); ($C_6H_4(COO)_2$) = terephthalate; DTBB = 2,2′-dithiobis(benzoate).

Synthesis and structural characterization of a barium coordination polymer based on a μ_2-monoatomic bridging 4-nitrobenzoate

Dedicated to Prof. A.V. Salker on the occasion of his 63rd birthday

POOJA H BHARGAO and BIKSHANDARKOIL R SRINIVASAN*
School of Chemical Sciences, Goa University, Goa 403 206, India
Email: srini@unigoa.ac.in

Supplementary Material for ONLINE version

CONTENTS

Table S1 – Geometric parameters (Å, °) of the 4nba and NMF ligands.

C1-O4	1.258(5)	O4-C1-O3	124.4(4)
C1-O3	1.262(5)	O4-C1-C2	118.3(3)
C1-C2	1.512(5)	O3-C1-C2	117.3(3)
C2-C3	1.377(5)	C3-C2-C7	119.2(4)
C2-C7	1.385(5)	C3-C2-C1	120.6(4)
C3-C4	1.380(6)	C7-C2-C1	120.2(3)
C4-C5	1.362(7)	C2-C3-C4	120.9(4)
C5-C6	1.371(6)	C5-C4-C3	118.8(4)
C5-N2	1.477(6)	C4-C5-C6	122.3(4)
C6-C7	1.389(6)	C4-C5-N2	118.5(4)
C8-O5	1.227(5)	C6-C5-N2	119.2(4)
C8-N1	1.304(6)	C5-C6-C7	118.4(4)
C9-N1	1.444(6)	C2-C7-C6	120.4(4)
N2-O1	1.173(6)	O5-C8-N1	125.2(4)
N2-O2	1.189(6)	C8-N1-C9	121.9(4)
O1-N2-C5	118.8(5)	O1-N2-O2	122.1(5)
		O2-N2-C5	119.1(5)

Table S2 – Hydrogen bonding geometry [Å and [°] for **1**.

D-H···A	d(D-H)	d(H···A)	d(D···A)	<DHA	Symmetry code
Interchain interactions					
C4-H4···O1	0.93	2.51	3.224(7)	134.2	-x+1/2, -y, z-1/2
N1-H1A···O4	0.847(19)	2.15(2)	2.981(5)	169(5)	x-1/2, y, -z-1/2
Intrachain interactions					
C8-H8···O6	0.93	2.57	3.124(6)	118.7	x, y, z
O7-H7A···O4	0.821(18)	2.16(2)	2.959(4)	166(4)	x-1,-y+1/2, z
O6-H6A···O4	0.860(19)	1.97(2)	2.815(4)	166(6)	x, -y+1/2, z

D= Donor and A= Acceptor

Figure S1 – Crystals of compound **1**

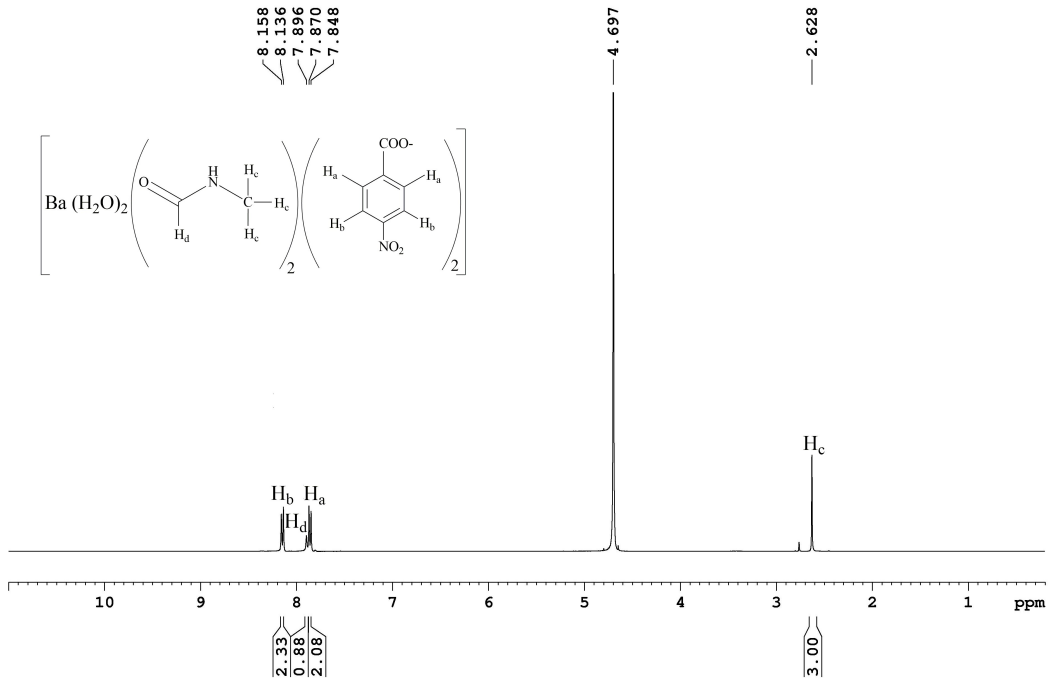

Figure S2 – ^{1}H NMR spectrum of **1** in D_2O.

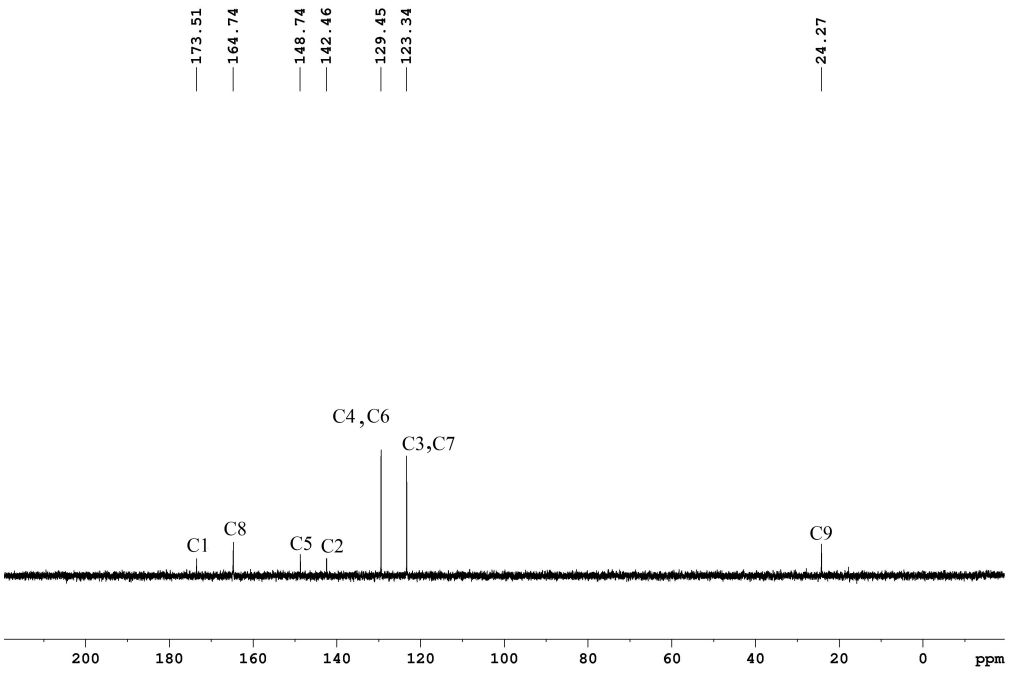

Figure S3 –^{13}C NMR spectrum of compound **1**. The assignments of the carbon signals are as in the crystal structure (Figure 1).

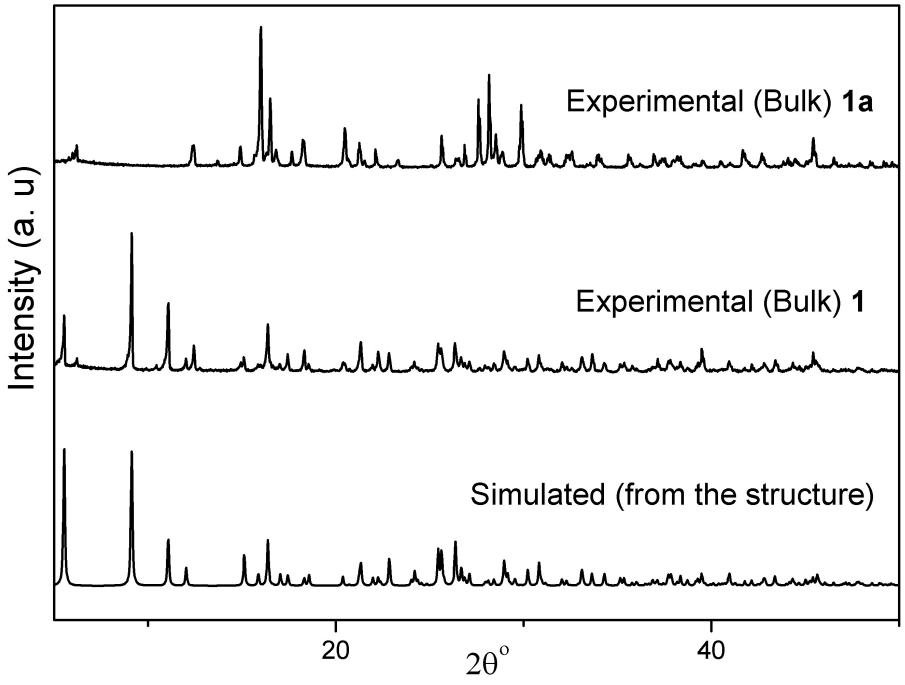

Figure S4 –Powder X-ray pattern of **1** and **1a**.

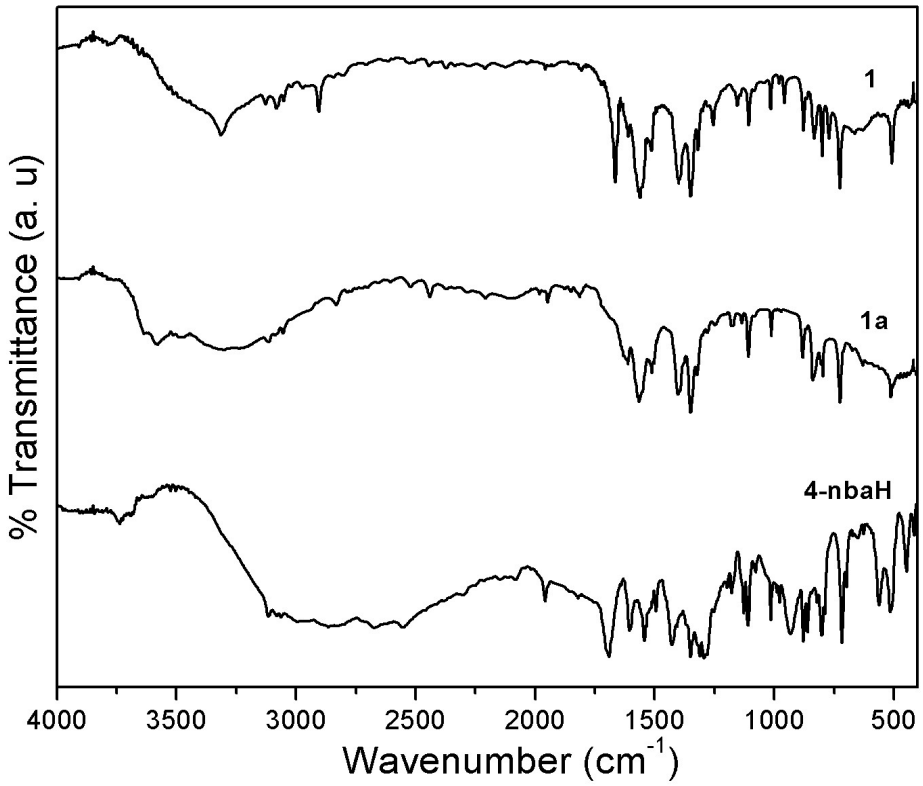

Figure S5 – Infrared spectra of **1**, **1a** and free ligand 4-nbaH

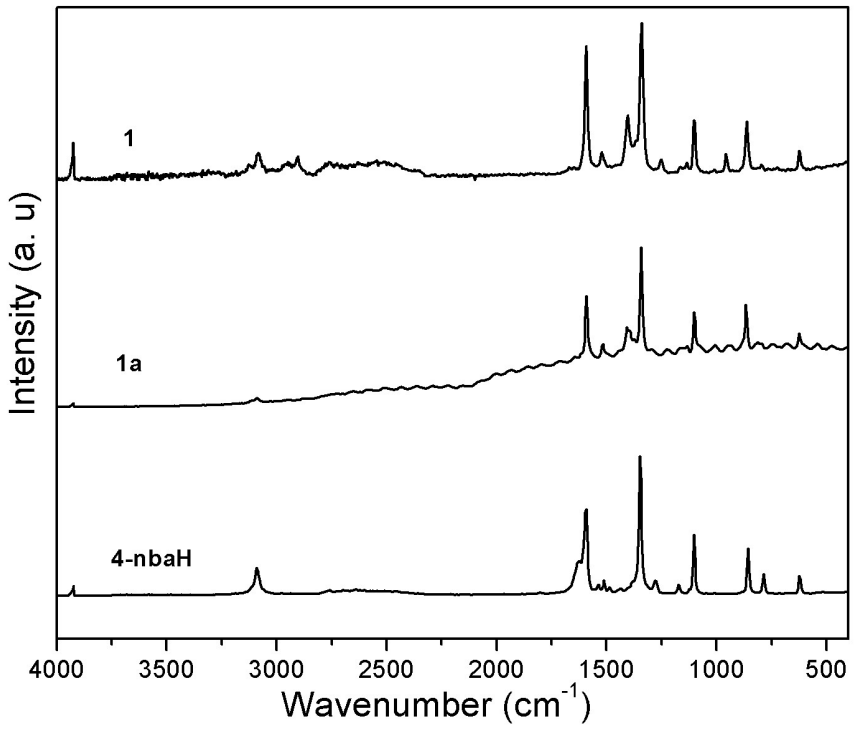

Figure S6 – Raman spectra of **1**, **1a** and the free ligand 4-nbaH.

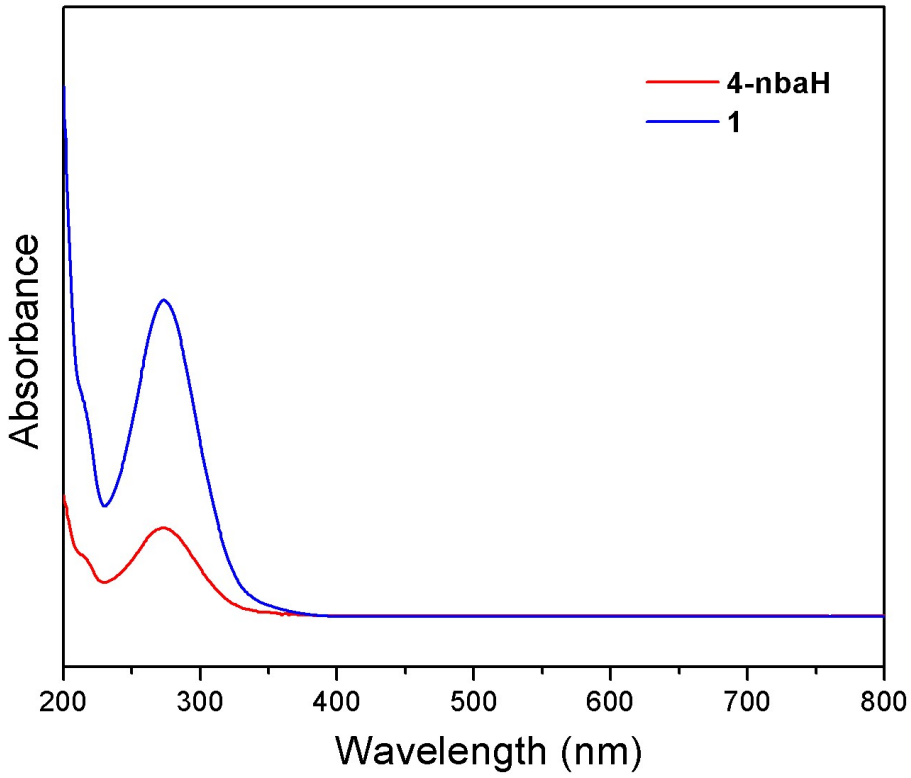

Figure S7 – UV-Visible spectra of **1** and free ligand 4-nbaH in water.

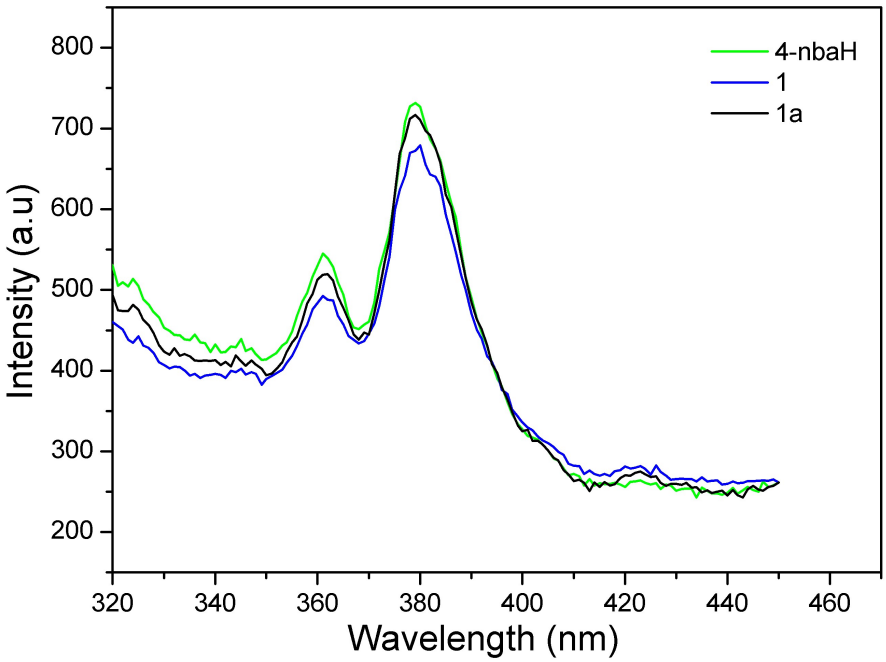

Figure S8 – Solid state photoluminescence spectra of the ligand 4-nbaH (green), **1a** (black) and **1** (blue).

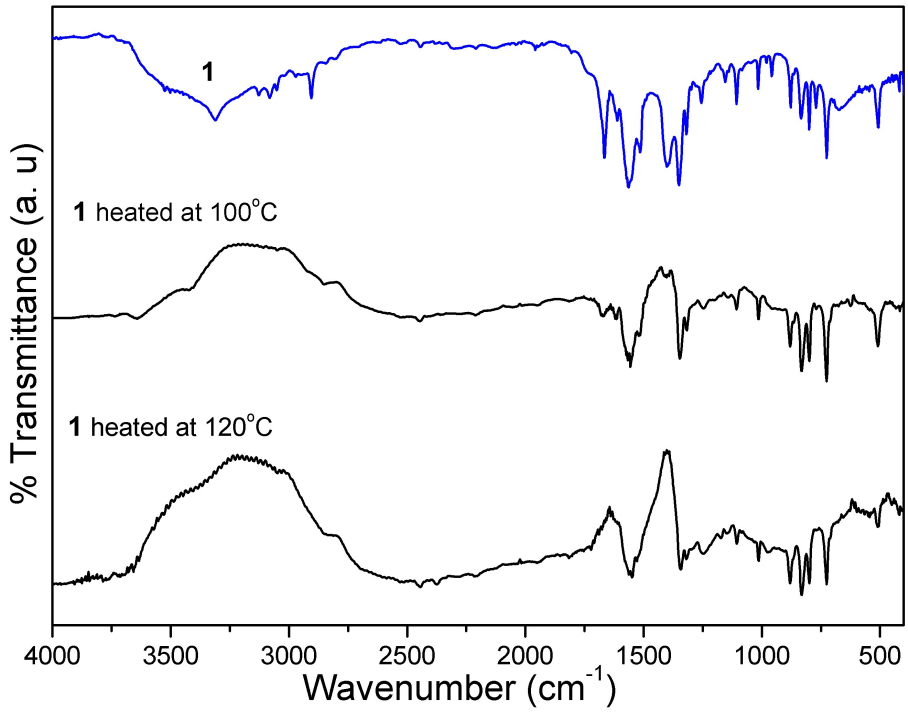

Figure S9 – IR spectra of **1** after heating at 100ºC (**Middle**) and 120ºC (**Bottom**).

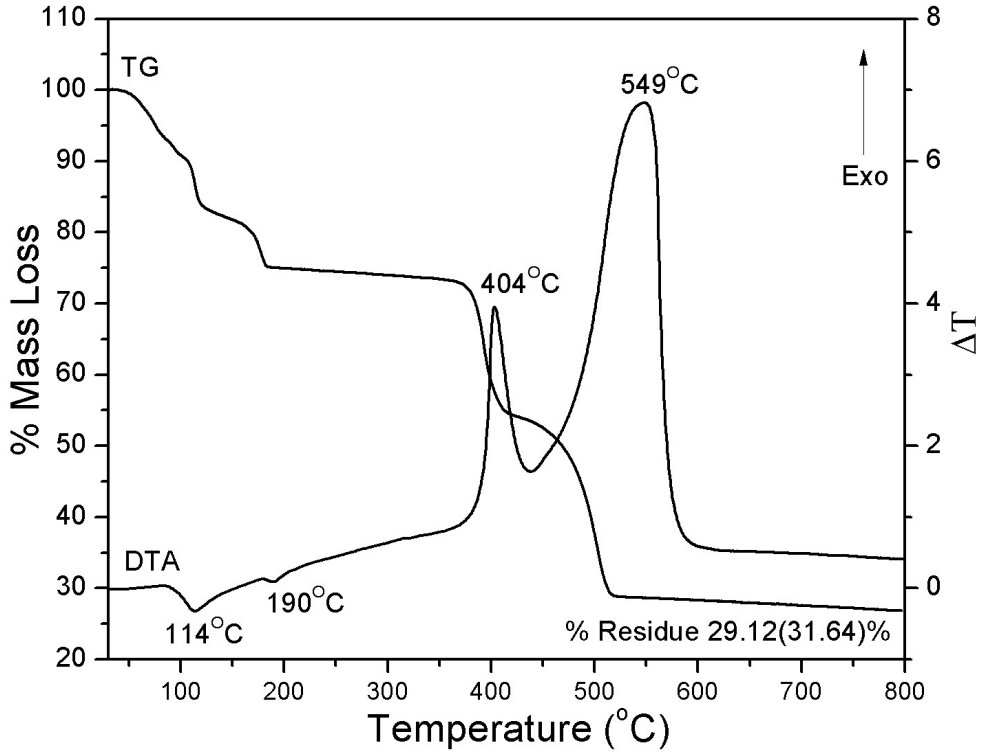

Figure S10 – TG-DTA curves of **1** in air atmosphere (Heating rate 10K / min)

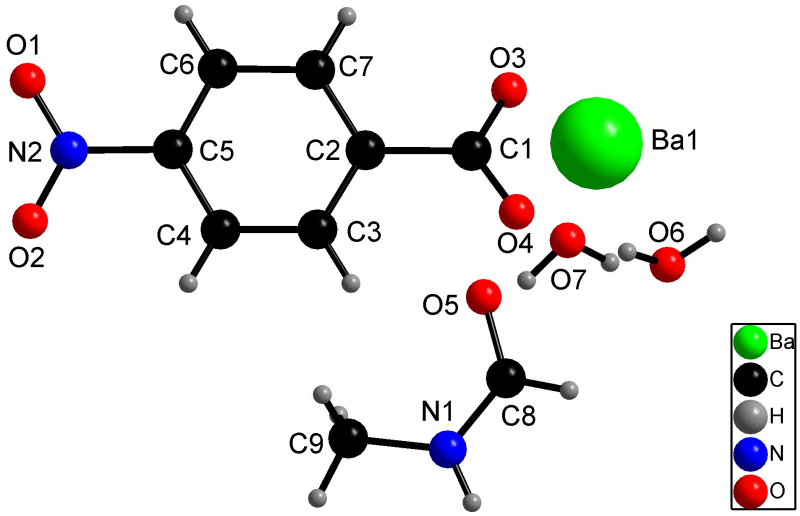

Figure S11– The asymmetric unit of $[Ba(H_2O)_2(NMF)_2(4\text{-nba})_2]$ (**1**)

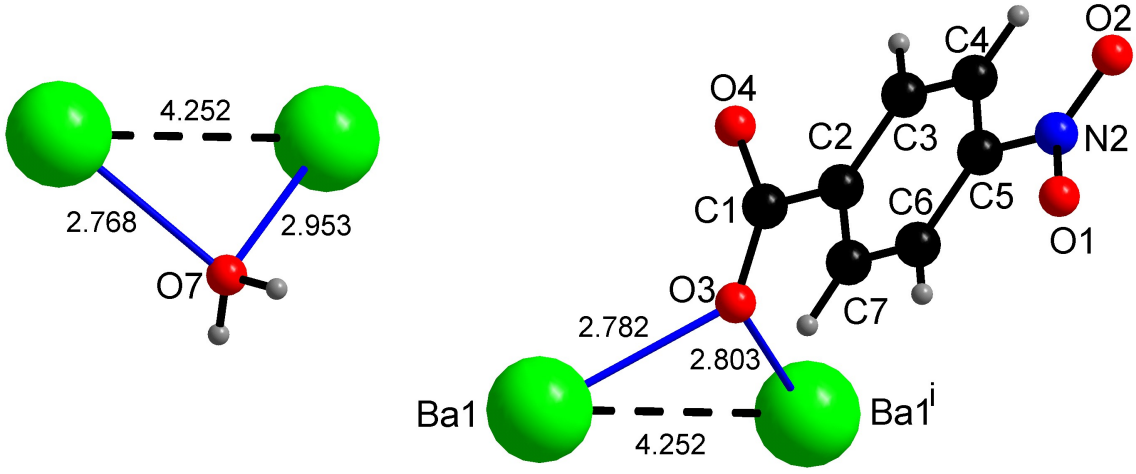

Figure S12 – Binding modes of the bridging ligands water O7 (left) and 4-nba (right) in **l**.

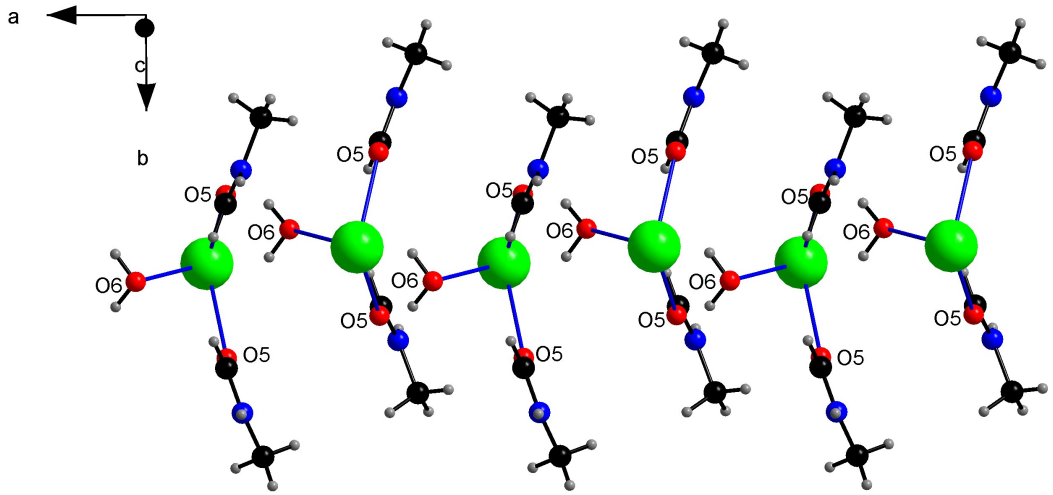

Figure S13 – A view of the crystal structure along *c* axis showing the terminal ligands (water (O6) and NMF (O5) in **1**. For clarity, the bridging 4-nba ligand and bridging aqua ligand (O7) around each Ba(II) are not displayed.

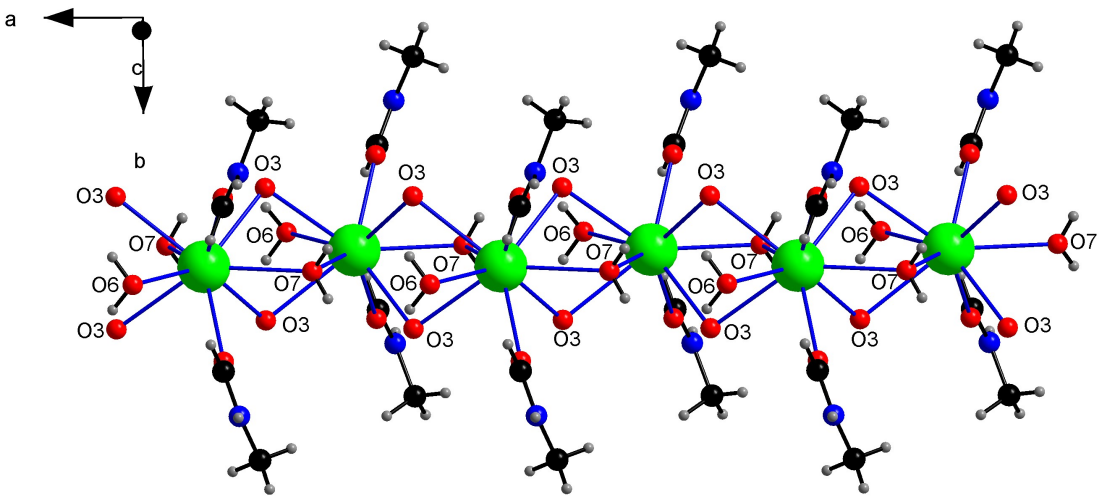

Figure S14 –A view along *c* axis showing the triple chain in **1**. Ba-O linkages are in blue. For clarity, only the H atoms of O6 and O7 are displayed. For the bridging 4-nba ligand only the bridging O3 atom is shown.

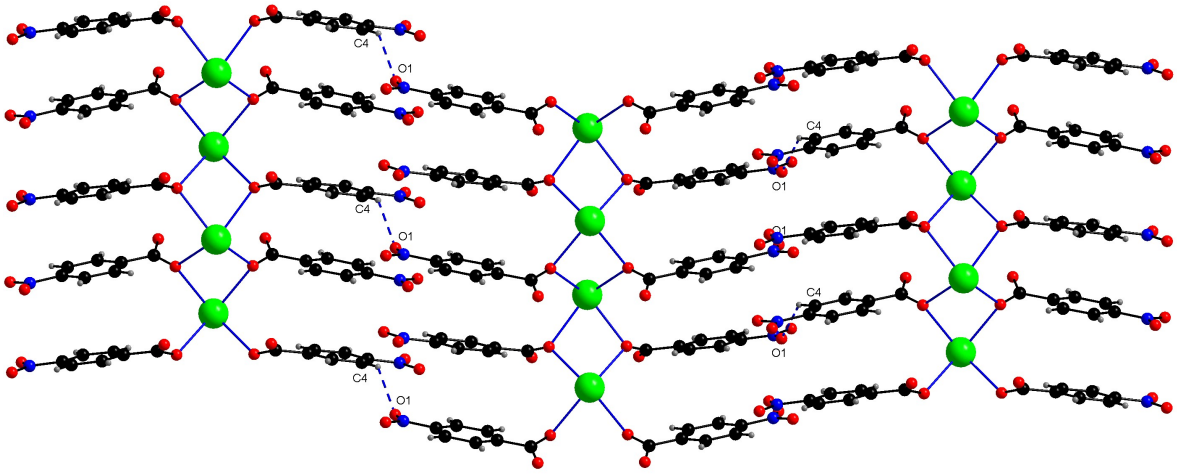

Figure S15 – A view of the crystal structure showing the linking of adjacent chains via the C4-H4···O1 interactions in **1**. For clarity, only the bridging 4-nba ligands around Ba are shown, and the other ligands are not displayed.

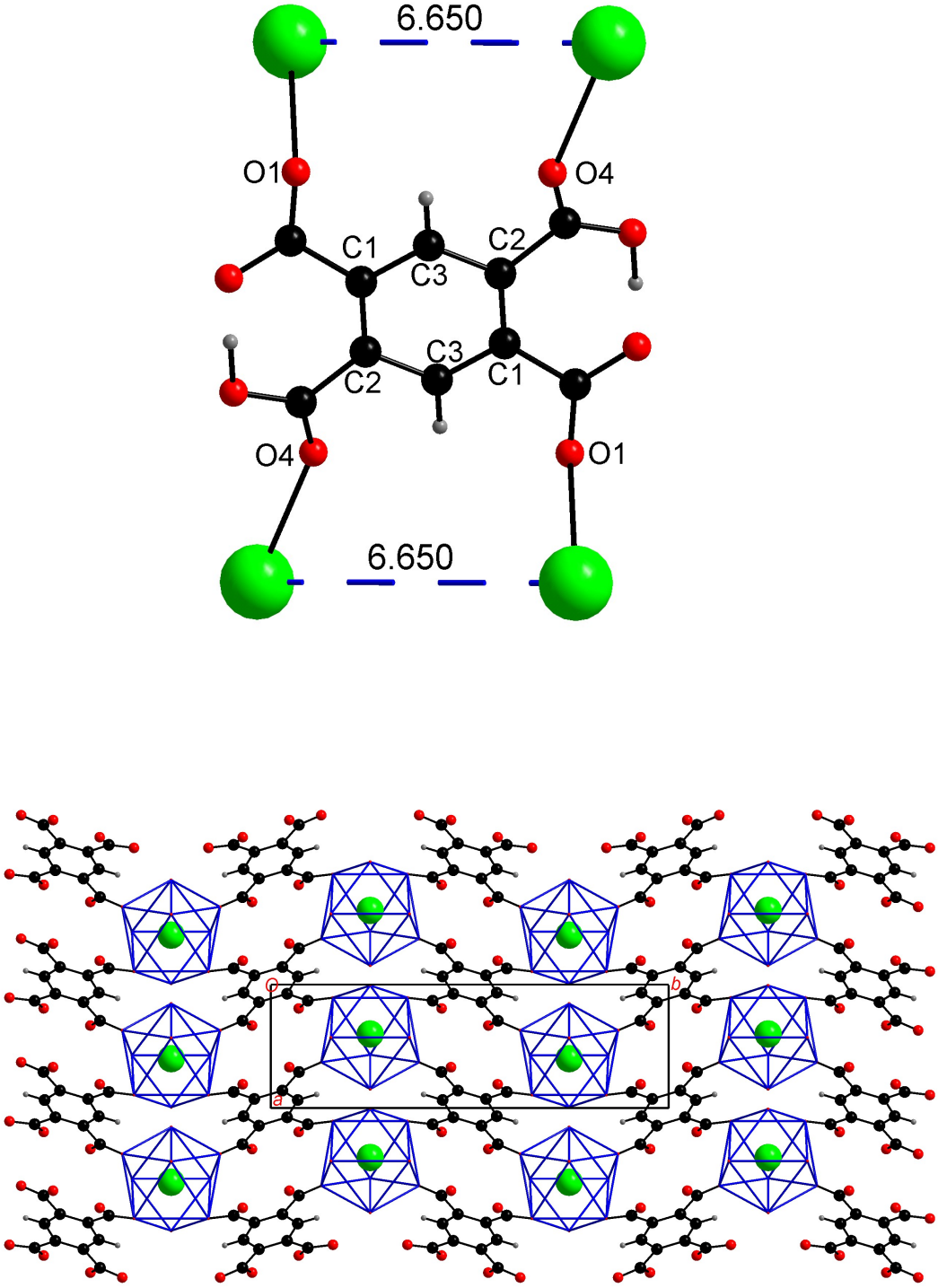

Figure S16– Binding mode (**top**) of the dianion of pyromellitic acid (H_2PMA). Each (H_2PMA) ligand is linked to four {BaO_9} polyhedra in the 2D compound (entry No. 24 in Table 3) [$Ba(H_2PMA)(H_2O)_5$] (**bottom**). Above figure is drawn using CIF file from Ref. 57.

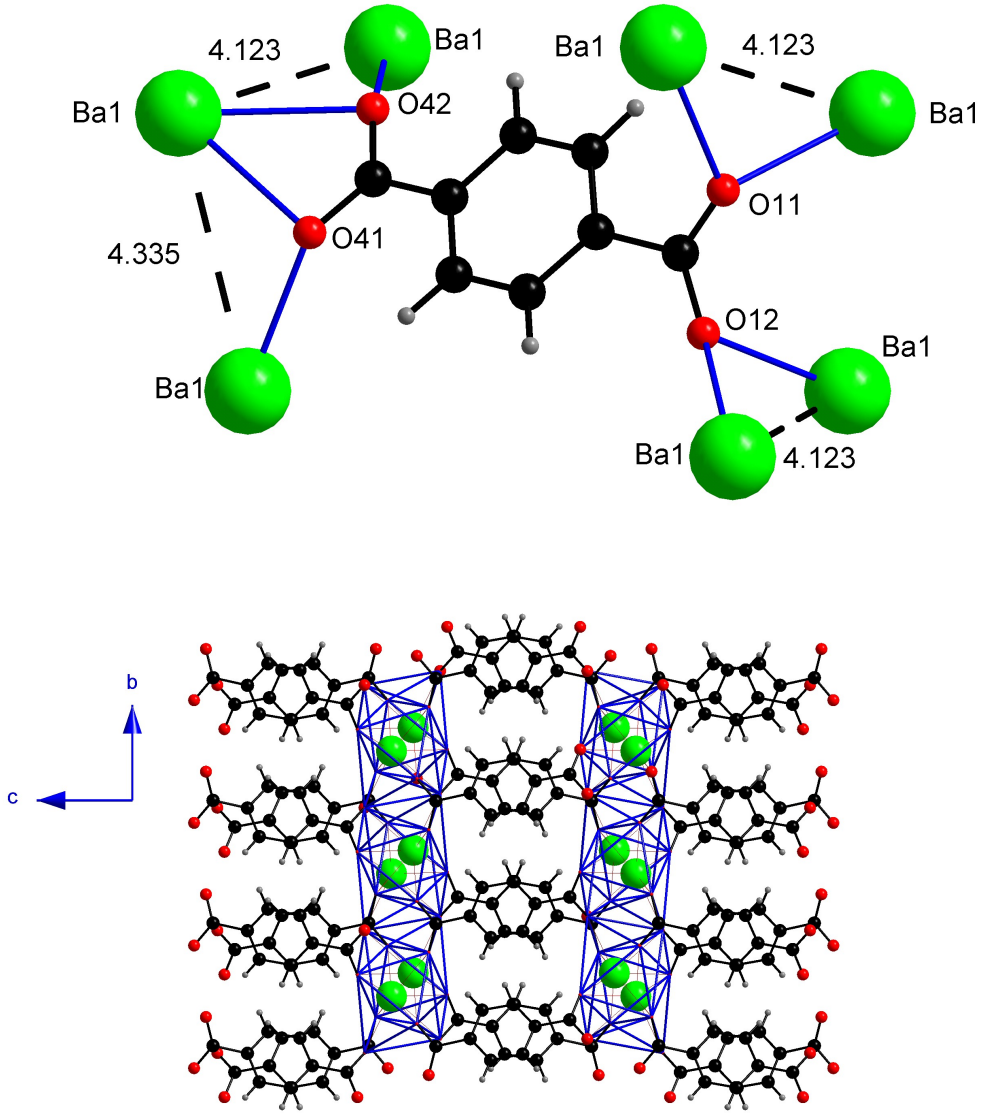

Figure S17 – The μ_7-octadentate binding mode in the three-dimensional barium terephthalate compound (entry No. 57 in Table 3)showing the different Ba···Ba separations (top). A view along a axis showing the face sharing $\{BaO_8\}$ polyhedra for which the aromatic acid linker functions like a scaffold. Figure is drawn using the CIF file from Ref. 60.